



*Supplement of*

## **Reconstructing burnt area during the Holocene: an Iberian case study**

**Yicheng Shen et al.**

*Correspondence to:* Yicheng Shen (yicheng.shen@pgr.reading.ac.uk)

The copyright of individual parts of the supplement might differ from the article licence.

This SI contains the following sections: (1) the Canonical Correlation Analysis (CCA) of modern pollen assemblages (2) information about the preparation of the Iberian pollen data, (3) information about the Iberian charcoal data, (4) the analyses used to select the final GLM, (5) Box-Cox transformation of palaeo burnt area fraction, (6) testing of the impact of using of micro and macro charcoal on the burnt area fraction reconstructions, and (7) comparisons of the fxTWA-PLS reconstructions 5 with reconstructions based on alternative methods (WA-PLS, TWA-PLS).

This SI includes the following Figures and Tables:

**Figure S1.** Partial correlations test based on data sets for the Iberian Peninsula that include annual observations at 0.5° for the period between 2001 and 2016. The data are all transformed according to Table S5 prior to the test.

10 **Figure S2.** Partial residual plots of the final model (Table S6, last column). The plot includes (1) the expected value (blue line); (2) a confidence interval for the expected value (grey band); (3) partial residuals (dark grey dots).

**Figure S3.** Distribution of palaeo burnt area fraction before (Panel A) and after (Panel B) Box-Cox transform.

15 **Figure S4.** Composite plots for macroscopic and microscopic charcoal separately of 16 charcoal sites with both macroscopic and microscopic entities using the locfit() function with half-width=300, number of bootstrap samples=1000. The locally estimated scatterplot smoothing is shown in blue; The upper and lower 95th-percentile confidence intervals are shown in grey.

**Figure S5.** The fitted plots and residual plots of WA-PLS and TWA-PLS methods, with and without fx correction.

**Figure S6.** Composite curves of reconstructed burnt area using WAPLS and TWAPLS, with and without fx correction, using the locfit() function with half-width=300, number of bootstrap samples=1000. The locally estimated scatterplot smoothing is shown in blue; The upper and lower 95th-percentile confidence intervals are shown in grey.

20 **Table S1.** Canonical Correlation Analysis (CCA) of pollen data

**Table S2.** Information on the pollen records. Latitude: degrees decimal where +ve is N and -ve is S. Longitude: degrees decimal where +ve is E and -ve is W. Elevation: in metres above sea level. Source: EPD = European Pollen Database ([www.europeanpollendatabase.net](http://www.europeanpollendatabase.net)); PANGAEA = [www.pangaea.de/](http://www.pangaea.de/).

25 **Table S3.** Pollen taxa in the Iberian dataset (205 taxa). Pollen taxa used in deriving the fire-vegetation relationship and fire reconstructions are shown in bold (140 taxa).

**Table S4.** Information on the charcoal records. Latitude: degrees decimal where +ve is N and -ve is S. Longitude: degrees decimal where +ve is E and -ve is W. Elevation: in metres above sea level.

**Table S5.** Environmental variables and transformation methods

30 **Table S6.** The process of the model selection. Regression coefficients (t value) and pseudo-R<sup>2</sup> of each model are shown. The final model is shown in bold.

**Table S7.** Results of fxTWAPLS using different values of  $\lambda$ .

**Table S8.** Leave-out cross-validation fitness of WA-PLS and TWA-PLS methods, with and without fx correction, showing

## S1. Canonical Correspondence Analysis (CCA) of the environmental controls on pollen assemblages

The central premise of our approach is that fire is *one* of the factors that modify vegetation assemblages, and therefore that differences in vegetation assemblages can be used to reconstruct fire. We used Canonical Correspondence Analysis (CCA) to investigate how much of the variation in modern pollen assemblages could be explained by burnt area alone, as compared to how much could be explained by burnt area combined with other environmental factors. We used the eight environmental factors considered in our generalised linear model (GLM) for this second analysis, specifically diurnal temperature range, dry days per month, wind speed, gross primary production, non-tree cover, cropland, grazing land, and urban population density. The CCA (Table S1) shows that *ca* 18% of the observed variability in the pollen assemblages is explained by the combination of these environmental variables and burnt area, and that burnt area alone explains *ca* 1% of the variability. Thus, the pollen assemblages contain specific information needed to reconstruct burnt area, even though other environmental influences have larger effects.

45 **Table S1.** Canonical Correspondence Analysis (CCA) of pollen data

CCA (a) – burnt area and other environmental variables		
	Inertia	Proportion explained
Total	6.129	1.0000
Constrained	1.113	0.1815
Unconstrained	5.016	0.8185

CCA (b) – burnt area only		
	Inertia	Proportion explained
Total	6.129	1.0000
Constrained	0.054	0.0088
Unconstrained	6.075	0.9912

## S2. Preparation of the Iberian pollen data

Table S2 provides information about the Iberian pollen sites:

**Table S2.** Information on the pollen records. Latitude: degrees decimal where +ve is N and -ve is S. Longitude: degrees decimal where +ve is E and -ve is W. Elevation: in metres above sea level. Source: EPD = European Pollen Database ([www.europeanpollendatabase.net](http://www.europeanpollendatabase.net)); PANGAEA = [www.pangaea.de/](http://www.pangaea.de/).

Site name	Entity	Source	Latitude	Longitude	Elevation	Reference
Almenara de Adaja	ADAJA	EPD	41.19	-4.67	784	(López Merino et al., 2009)
Alsa	ALSA	EPD	43.12	-4.02	560	(Mariscal, 1993)
Alvor Estuary Ribeira do Farelo Ribeira da Torre	Abi 05/07	author	37.15	-8.59	0.6	(Schneider et al., 2010, 2016)
Antas	ANTAS	EPD	37.21	-1.82	0	(Cano Villanueva, 1997; Pantaléon-Cano et al., 2003; Yll et al., 1995)
Arbarrain Mire	ARBARRAIN	author	43.21	-2.17	1004	(Pérez-Díaz et al., 2018)
Armacao de Pera Ribeira de Alcantarilha	ADP 01/06	author	37.11	-8.34	2.4	(Schneider et al., 2010, 2016)
Armena	Armena	author	42.51	0.34	2238	(Leunda et al., 2019)
Arroyo de Aguas Frias	AGUASFRIAS	author	40.27	-5.12	1120	(Julio Camarero et al., 2019)
Arroyo de las Cárcavas	CARCAVAS	EPD	40.84	-4.03	1300	(Morales-Molino et al., 2017a)
Arroyo de Navalacarreta	NAVALACA	EPD	40.85	-4.03	1250	(Morales-Molino et al., 2017a)
Arroyo de Valdeconejos	VALDECON	EPD	40.86	-4.06	1380	(Morales-Molino et al., 2017a)
Atxuri	ATXURI01	EPD	43.25	-1.55	500	(Penalba, 1994; Penalba and Garmendia, 1989)
Ayoó de Vidriales	AYOO	EPD	42.13	-6.07	780	(Morales-Molino and García-Antón, 2014)
Basa de la Mora	BSM08	author	42.55	0.33	1906	(Pérez-Sanz et al., 2013)
Bassa Nera	BSN6	author	42.64	0.92	1891	(Garcés-Pastor et al., 2017)
Bermu Mire	BERMU	author	39.43	-4.15	783	(Luelmo-Lautenschlaeger et al., 2018c)
Borreguil de la Caldera	BdIC-01	author	37.05	-3.32	2992	(Ramos-Román et al., 2016)

Bosc dels Estanyons	BOSCESTA	EPD	42.48	1.63	2180	(De Beaulieu et al., 2005; Miras et al., 2007)
Botija Bog	BOTIJA	author	39.60	-4.70	755	(Luelmo-Lautenschlaeger et al., 2018b)
Campo Lameiro	PRD4	EPD	42.53	-8.52	260	(Kaal et al., 2011; López-Merino et al., 2012; Kaal et al., 2013)
Canada de la Cruz	CANCRUZ	EPD	38.07	-2.69	1595	(Carrión et al., 2001)
Canada del Gitano _ Sierra de Baza	SBAZA	EPD	37.23	-2.70	1900	(Carrión et al., 2007)
Canaleja	CANALEJA	EPD	40.90	-2.45	1029	(Cerrillo Cuenca et al., 2007; Cerrillo Cuenca and González Cordero, 2011)
Castello Lagoon	Castello Lagoon core EM	author	42.28	3.10	2.4	(Ejarque et al., 2016)
Cha das Lameiras	LAMEIRAS	author	40.94	-7.68	950	(López-Sáez et al., 2017)
Charco da Candieira	CANDIEIR	EPD	40.34	-7.58	1409	(van der Knaap and van Leeuwen, 1984, 1995, 1997)
Creixell	CreixellT	EPD	41.16	1.43	1	(Burjachs and Expósito, 2015)
Cucú cueva	CUCU	EPD	37.64	-2.26	1600	(González-Ramón et al., 2012)
Cueto de la Avellanosa	CUETOAV	EPD	43.12	-4.36	1320	(Mariscal Alvarez, 1983)
Culazón	CULAZON	EPD	43.23	-4.49	592	(López-Sáez et al., 2013)
Elx	ELX	EPD	38.17	-0.75	1	(Burjachs et al., 1997; Burjachs and Expósito, 2015)
El Brezosa	BREZOSA	author	39.35	-4.36	733	(Morales-Molino et al., 2018)
El Carrizal	CARRIZAL	EPD	41.32	-4.15	860	(Franco-Múgica et al., 2005)
El Maíllo mire	MAI	EPD	40.55	-6.21	1100	(Morales-Molino et al., 2013)
El Payo	ELPAYO	EPD	40.25	-6.77	1000	(Abel-Schaad et al., 2009b; Silva-Sánchez et al., 2016)
El Perro mire	ELPERRO	author	39.05	-4.76	690	(Luelmo-Lautenschlaeger et al., 2019a, 2019b)
El Portalet	PORTALET	author	42.80	-0.40	1802	(González-Sampériz et al., 2006)
El Redondo	REDONDO	author	40.22	-5.66	1765	(López-Sáez et al., 2016b)
El Sabinar	SABINAR	EPD	38.20	-2.12	1117	(Carrión et al., 2004)
El Tiemblo	TIEMBLO	author	40.36	-4.53	1250	(López-Sáez et al., 2018b)

Enol	ENOL	author	43.27	-4.99	1075	(Moreno et al., 2011)
Espinosa de Cerrato	CERRATO	author	41.96	-3.94	885	(Morales-Molino et al., 2017b; Múgica et al., 2001)
Estanilles	ESTANILLES	EPD	42.63	1.30	2247	(Pérez-Obiol et al., 2012)
Estanya	Estanya Catena	author	42.03	0.53	677	(González-Sampériz et al., 2017; Morellón et al., 2011)
Fuente de la Leche	LECHE	author	40.35	-5.06	1382	(Robles-López et al., 2018)
Fuente del Pino Blanco	PINOBLANCO	author	40.24	-4.98	1343	(Robles-López et al., 2018)
Hinojos Marsh	HINOJOS	author	36.96	-6.39	1.5	(López-Sáez et al., 2018a)
Hoya del Castillo	N-CAS	EPD	41.48	-0.16	258	(Davis and Stevenson, 2007)
La Cruz	LACRUZ	EPD	39.99	-1.87	1024	(Burjachs et al., 1997)
La Molina mire	MOLINAES	author	43.38	-6.33	650	(López-Merino et al., 2011)
Labradillos Mire S	LABRADILLO S	author	40.34	-4.57	1460	(Robles-López et al., 2017)
Lago de Ajo	LAGOAJO	EPD	43.05	-6.15	1570	(Allen et al., 1996; McKeever, 1984)
Lagoa Comprida 2	LAGOA_CO	EPD	40.36	-7.64	1650	(Van Den Brink and Janssen, 1985; Janssen and Woldringh, 1981; Moe and Van Der Knaap, 1990)
Laguna de la Mosca	LdlMo composite	author	37.06	-3.31	2889	(Manzano et al., 2019)
Laguna de la Mula	LdlM 10-02	author	37.06	-3.42	2497	(Jiménez-Moreno et al., 2013)
Laguna de la Roya	LAROYA	PANGA EA	42.22	-6.77	1608	(Allen et al., 1996)
Laguna de Rio Seco	Laguna de Rio Seco core 1	author	37.05	-3.35	3020	(Anderson et al., 2011)
Laguna Guallar	N-GUA	EPD	41.41	-0.23	336	(Davis and Stevenson, 2007)
Laguna Mesagosa	LAGMESAG	EPD	41.97	-2.81	1600	(Engelbrechten, 1999)
Laguna Negra	LAGNEGRA	EPD	42.00	-2.85	1760	(Engelbrechten, 1999)
Laguna Salada Chiprana	N-SAL	EPD	41.23	-0.17	150	(Valero-Garcés et al., 2000)
Lake Banyoles	Banyoles SB2	EPD	42.13	2.75	174	(Revelles et al., 2015)
Lake Banyoles	BANYOLES_1	EPD	42.13	2.75	174	(Pérez-Obiol and Julià, 1994)
Lake Saloio	SALOIO	EPD	39.61	-9.02	70	(Gomes, 2011)
Lanzahíta	LANZBOG	author	40.22	-4.94	558	(López-Sáez et al., 1999, 2010)

Las Animas Mire	ANIMAS	author	36.69	-5.03	1403	(Alba-Sánchez et al., 2019)
Las Lanchas	LANCHAS	author	39.59	-4.89	800	(Luelmo-Lautenschlaeger et al., 2018a)
Las Pardillas	LASPARDI	EPD	42.03	-3.03	1850	(Sanchez Goñi and Hannon, 1999)
Las Vinuelas	VINUELAS	author	39.37	-4.49	761	(Morales - Molino et al., 2019)
Les Palanques	PALANQUES	EPD	42.16	2.44	460	(Revelles et al., 2018)
Manaderos	Manaderos core	author	40.34	-4.69	1292	(Robles-López et al., 2020)
Marbore	Marbore composite	author	42.70	0.04	2612	(Leunda et al., 2017)
Monte Areo mire	AREO	EPD	43.53	-5.77	200	(López-Merino et al., 2010)
Montes do Buio Cuadramón	CUAII	EPD	43.47	-7.53	700	(González and Saa, 2000)
Navamuno	Navamuno_S3	author	40.32	-5.78	1505	(López-Sáez et al., 2020)
Navarrés	NAVA1	EPD	39.10	-0.68	225	(Carrión and Dupre, 1996)
Navarrés	NAVARRE3	EPD	39.10	-0.68	225	(Carrión and Van Geel, 1999)
Ojos del Tremendal	Ojos del Tremendal core 1	author	40.54	-2.05	1650	(Stevenson, 2000)
Patateros bog	PATATERO	EPD	39.60	-4.67	700	(Dorado-Valiño et al., 2014)
Pedrido	PEDRIDO	EPD	43.44	-7.07	770	(Stefanini, 2008)
Pena de Cadela	CADELA	EPD	42.83	-7.17	970	(Mighall et al., 2006)
Peña Negra	PENANEGR	EPD	40.33	-5.79	1000	(Abel-Schaad and López-Sáez, 2013)
Pico del Sertal	SERTAL	EPD	43.22	-4.44	940	(Mariscal Alvarez, 1986)
Pla de l'Estany	PLAESTANY	EPD	42.19	2.54	520	(Burjachs, 1994)
Planell de Perafita	PERAFITA	EPD	42.48	1.57	2240	(Miras et al., 2010)
Posidonia Lligat	LLIGAT	EPD	42.29	-3.29	-3	(López-Sáez et al., 2009)
Pozo de la Nieve	PozoN_2015 core	author	40.35	-4.55	1600	(Robles-López et al., 2017)
Prailllos de Bossier Mire	BOSSIER	EPD	36.91	-4.07	1610	(Abel-Schaad et al., 2017)
Puerto de Belate	BELATE01	EPD	43.03	-2.05	847	(Penalba, 1994; Penalba and Garmendia, 1989)
Puerto de las Estacas de Trueba	ESTACAS EA	PANGA	43.12	-3.70	1160	(Mariscal, 1989)
Puerto de Los Tornos	TORNOS01	EPD	43.15	-3.43	920	(Penalba and Garmendia, 1989)

Puerto de Serranillos	SERRANIL	EPD	40.31	-4.93	1700	(López-Merino et al., 2009)
Quintanar de la Sierra	QUINTA02	EPD	42.03	-3.02	1470	(Penalba, 1994; Penalba and Garmendia, 1989)
Roquetas de Mar	ROQUETAS	EPD	36.79	-2.59	0	(Cano Villanueva, 1997; Obiol and Roure, 1994; Pantaléon-Cano et al., 2003; Yll et al., 1995)
Salada Pequeña	N-PEQ	EPD	41.03	-0.22	357	(Davis, 2010)
Saldropo	SALDROPO	EPD	43.05	-2.72	625	(Penalba, 1994; Penalba and Garmendia, 1989)
Salines playa-lake	SALINES	EPD	38.50	-0.89	475	(Burjachs et al., 2017)
San Rafael	SANRAFA	EPD	36.77	-2.60	0	(Cano Villanueva, 1997; Pantaléon-Cano et al., 2003; Yll et al., 1995)
Sanabria Marsh	SANABRIA	EPD	42.10	-6.73	1050	(Allen et al., 1996; Hannon, 1985; Turner and Hannon, 1988)
Serra Mitjana Fen	MITJANA	EPD	42.47	1.58	2406	(Miras et al., 2015)
Serrania de las Villuercas	VILLUERCAS	author	39.48	-5.4	1000	(Gil-Romera et al., 2008)
Sierra de Gádor	GADOR	EPD	36.90	-2.92	1530	(Carrión et al., 2003)
Siles Lake	SILES	EPD	38.40	-2.50	1320	(Carrión, 2002)
Tubilla del Lago	TUB	EPD	41.81	-3.57	900	(Morales-Molino et al., 2017b)
Turbera de La Panera Cabras	PANERA	EPD	40.17	-5.76	1648	(Abel-Schaad et al., 2009a)
Valdeyernos bog	VALDEYER	EPD	39.44	-4.10	850	(Dorado-Valiño et al., 2014)
Valle do Lobo Ribeira de Carcavai	VdL PB2	author	37.06	-8.07	2.3	(Schneider et al., 2010, 2016)
Verdeospesoa mire OA	VERDEOSPES OA	author	43.06	-2.86	1015	(Pérez-Díaz and López-Sáez, 2017, 2019)
Vilamora Ribeira de Quarteira	Vilamora P01-5	author	37.09	-8.14	3.5	(Schneider et al., 2010, 2016)
Villarquemado		author	40.49	-1.29	985	(González-Sampériz et al., 2020; Valero-Garcés et al., 2019)
Villaverde	VILLAVERDE	EPD	38.80	-2.37	870	(Carrión et al., 2001b)
Xan de Llamas	XL	EPD	42.30	-6.32	1500	(Morales-Molino et al., 2011)
Zoñar	ZONARcombin ed	author	37.48	-4.69	300	(Martín-Puertas et al., 2008)

Non-pollen palynomorphs (e.g. fungi, algae), introduced species, and fire-insensitive plants (e.g. obligate aquatics) were removed before analysis on the assumption that these were not diagnostic of changing fire regimes. Some pollen taxa are not identified consistently by palynologists or occur at very few sites, so some pollen types were amalgamated to higher taxonomic groups (genera for trees, families for herbaceous taxa) for consistency across the records (Table S3).

**Table S3.** Pollen taxa in the Iberian dataset (205 taxa). Pollen taxa used in deriving the fire-vegetation relationship and fire reconstructions are shown in bold (140 taxa).

Taxon:

<b>Abies</b>	<b>Acer</b>	<b>Aconitum</b>	<b>Adonis</b>
Aesculus	Aizoaceae	<b>Alnus</b>	<b>Amaranthaceae</b>
<b>Amaryllidaceae</b>	Anacardiaceae	<b>Apiaceae</b>	<b>Aquilegia</b>
Araliaceae	<b>Arbutus</b>	Arctostaphylos	<b>Aristolochiaceae</b>
<b>Artemisia</b>	Asparagaceae	<b>Asphodelaceae</b>	<b>Asteraceae</b>
Asteraceae Liguliflorae	<b>Astroideae</b>	<b>Astragalus</b>	<b>Berberidaceae</b>
<b>Berberis</b>	<b>Betula</b>	Boraginaceae	<b>Brassicaceae</b>
<b>Buxus</b>	Calicotome	<b>Calluna</b>	<b>Campanulaceae</b>
<b>Caprifoliaceae</b>	<b>Carduoideae</b>	<b>Carpinus betulus</b>	Carpinus orientalis Ostrya
<b>Caryophyllaceae</b>	<b>Castanea</b>	<b>Cedrus</b>	<b>Celastraceae</b>
Celtis	Ceratonia	Chamaerops	<b>Cichorioideae</b>
<b>Cistaceae</b>	<b>Cistus</b>	Clematis	<b>Colchicaceae</b>
<b>Convolvulaceae</b>	Coriaria	Cornus	<b>Corylus</b>
<b>Crassulaceae</b>	<b>Crataegus</b>	Cucurbitaceae	<b>Cupressaceae</b>
<b>Cyperaceae</b>	Cytinaceae	<b>Daphne</b>	Delphinium
<b>Dennstaedtiaceae</b>	Dryas	Elaeagnus	<b>Empetrum</b>
<b>Ephedra</b>	Ephedraceae	<b>Equisetum</b>	<b>Erica</b>
<b>Ericaceae</b>	Eriocaulaceae	<b>Euphorbiaceae</b>	<b>Fabaceae</b>
<b>Fabaceae herbs</b>	<b>Fagus</b>	<b>Frangula</b>	<b>Fraxinus</b>
Genisteae	Gentianaceae	<b>Geraniaceae</b>	Grossulariaceae
Halimium	Haloragaceae	<b>Hedera</b>	<b>Helianthemum</b>
<b>Helleborus</b>	Hippophae	<b>Huperzia</b>	Hymenophyllaceae
<b>Hypericaceae</b>	<b>Ilex</b>	<b>Iridaceae</b>	Jasminum
Juglans	Juncaceae	Juncaginaceae	Koenigia
<b>Lamiaceae</b>	Larix	<b>Lavandula</b>	Ledum
Ligustrum	Liliaceae	<b>Linaceae</b>	Linnaea
<b>Linum</b>	<b>Lonicera</b>	Loranthaceae	<b>Lycopodium</b>
Lysimachia	Lythraceae	<b>Malvaceae</b>	Maytenus

<b>Melanthiaceae</b>	Mercurialis	Montiaceae	<b>Moraceae</b>
<b>Myrica</b>	<b>Myrtaceae</b>	<b>Nartheciaceae</b>	Nerium
Nigella	Olea	Oleaceae	<b>Onagraceae</b>
<b>Ononis</b>	<b>Ophioglossaceae</b>	Orchidaceae	<b>Orobanchaceae</b>
<b>Osmundaceae</b>	Oxalidaceae	<b>Oxyria Rumex</b>	<b>Paeonia</b>
<b>Papaveraceae</b>	Parrotia	Periploca	<b>Phillyrea</b>
<b>Picea</b>	Pinus	<b>Pinus diploxylon</b>	Pinus haploxyロン
<b>Pistacia</b>	<b>Plantaginaceae</b>	Platanus	<b>Plumbaginaceae</b>
<b>Poaceae</b>	<b>Polemoniaceae</b>	<b>Polygonaceae</b>	<b>Polygonaceae</b>
<b>Polygonum</b>	<b>Polypodiales</b>	Populus	Portulacaceae
<b>Potentilla</b>	<b>Primulaceae</b>	Prunus	<b>Pteridaceae</b>
Pterocarya	<b>Quercus deciduous</b>	<b>Quercus evergreen</b>	<b>Quercus intermediate</b>
<b>Ranunculaceae</b>	<b>Ranunculus</b>	<b>Resedaceae</b>	Retama
Rhamnaceae	<b>Rhamnus</b>	Rhododendron	Rhus
<b>Ribes</b>	<b>Rosaceae</b>	Rosmarinus	<b>Rubiaceae</b>
<b>Rubus</b>	Rutaceae	<b>Salix</b>	<b>Sambucus</b>
<b>Sanguisorba group</b>	Santalaceae	Sapotaceae	<b>Saxifragaceae</b>
Sciadopityaceae	<b>Scrophulariaceae</b>	Smilax	<b>Solanaceae</b>
<b>Sorbus</b>	Tamarix	Taxaceae	<b>Taxus</b>
<b>Teucrium</b>	<b>Thalictrum</b>	<b>Thymelaeaceae</b>	<b>Tilia</b>
Trollius	<b>Ulmus</b>	Ulmus Zelkova	<b>Urticaceae</b>
<b>Vaccinium</b>	<b>Valerianaceae</b>	Verbenaceae	<b>Viburnum</b>
<b>Violaceae</b>	Viscum	Vitex	<b>Ziziphus</b>
Zygophyllaceae			

### S3. Information about the Iberian charcoal data

**Table S4.** Information on the charcoal records. Latitude: degrees decimal where +ve is N and –ve is S. Longitude: degrees decimal where +ve is E and –ve is W. Elevation: in metres above sea level.

Site name	Entity name	Latitude	Longitude	Elevation	Reference
Alvor Estuary Ribeira do Farelo Ribeira da Torre	Abi 05_07_100minus	37.15	-8.59	0.6	(Schneider et al., 2010, 2016)
Alvor Estuary Ribeira do Farelo Ribeira da Torre	Abi 05_07_100plus	37.15	-8.59	0.6	(Schneider et al., 2010, 2016)
Arbarrain Mire	Arbarrain Mire core	43.21	-2.17	1004	(Pérez-Díaz et al., 2018)
Armacao de Pera Ribeira de Alcantarilha	ADP 01/06_100minus	37.11	-8.34	2.4	(Schneider et al., 2010, 2016)
Armacao de Pera Ribeira de Alcantarilha	ADP 01/06_100plus	37.11	-8.34	2.4	(Schneider et al., 2010, 2016)
Arroyo de Aguas Frias	Aguas Frias core	40.27	-5.12	1120	(Julio Camarero et al., 2019)
Arroyo de las Carcavas	Arroyo de las Carcavas core	40.84	-4.03	1300	(Morales-Molino et al., 2017a)
Arroyo de Valdeconejos	VALDECON	40.86	-4.06	1380	(Morales-Molino et al., 2017a)
Basa de la Mora	BSM08	42.55	0.33	1906	(Pérez-Sanz et al., 2013)
Bermu Mire	Bermu Mire core_large	39.43	-4.15	783	(Luelmo-Lautenschlaeger et al., 2018c)
Bermu Mire	Bermu Mire core_small	39.43	-4.15	783	(Luelmo-Lautenschlaeger et al., 2018c)
Borreguil de la Caldera	BdIC-01	37.05	-3.32	2992	(Ramos-Román et al., 2016)
Campo Lameiro	PRD4	42.53	-8.52	260	(Kaal et al., 2008)
Canada de la Cruz	Canada de la Cruz core	38.07	-2.69	1595	(Carrión et al., 2001a)
Canada del Gitano_Sierra de Baza	Baza section	37.23	-2.70	1900	(Carrión et al., 2007)
Castello Lagoon	Castello Lagoon core EM	42.28	3.10	2.4	(Ejarque et al., 2016)
Cha das Lameiras	Cha das Lameiras soil profile_macro	40.94	-7.68	950	(López-Sáez et al., 2017)

Cha das Lameiras	Cha das Lameiras soil profile_micro	40.94	-7.68	950	(López-Sáez et al., 2017)
Charco da Candieira	Candieira (Charco da Candieira) core	40.34	-7.58	1409	(Connor et al., 2012; van der Knaap and van Leeuwen, 1995, 1997)
Cubelles	Cubelles core	41.20	-1.67	2	(Riera-Mora and Esteban-Amat, 1994)
El Brezosa	El Brezosa core_macro	39.35	-4.36	733	(Morales-Molino et al., 2018)
El Brezosa	El Brezosa core_micro	39.35	-4.36	733	(Morales-Molino et al., 2018)
El Carrizal	El Carrizal core	41.32	-4.15	860	(Franco-Múgica et al., 2005)
El Perro mire	El Perro mire core	39.05	-4.76	690	(Luelmo-Lautenschlaeger et al., 2019a, 2019b)
El Portalet	PORTALET_macro	42.80	-0.40	1802	(González-Sampériz et al., 2006)
El Portalet	PORTALET_micro	42.80	-0.40	1802	(González-Sampériz et al., 2006)
El Redondo	El Redondo core o125	40.22	-5.66	1765	(López-Sáez et al., 2016b)
El Redondo	El Redondo core u125	40.22	-5.66	1765	(López-Sáez et al., 2016b)
El Tiemblo	El Tiemblo core	40.36	-4.53	1250	(López-Sáez et al., 2018b)
Espinosa de Cerrato	Espinosa de Cerrato core	41.96	-3.94	885	(Morales-Molino et al., 2017b)
Fuente de la Leche	Fuente de la Leche core	40.35	-5.06	1382	(Robles-López et al., 2018)
Fuente del Pino Blanco	FPB core	40.24	-4.98	1343	(Robles-López et al., 2018)
Hinojos Marsh	Hinojos Marsh_core S1_macro	36.96	-6.39	1.5	(López-Sáez et al., 2018a)
Hinojos Marsh	Hinojos Marsh_core S1_micro	36.96	-6.39	1.5	(López-Sáez et al., 2018a)
Hoya del Castillo	Hoya del Castillo N-CAS	41.48	-0.16	258	(Davis and Stevenson, 2007)
Hoya del Castillo	Hoya del Castillo N-CAS macro	41.48	-0.16	258	(Davis and Stevenson, 2007)
Laguna de la Mosca	LdlMo composite	37.06	-3.31	2889	(Manzano et al., 2019)

Laguna de la Mula	LdlM 10-02	37.06	-3.42	2497	(Jiménez-Moreno et al., 2013)
Laguna de Rio Seco	Laguna de Rio Seco core	37.05	-3.35	3020	(Anderson et al., 2011)
Laguna Guallar	N-GUA_macro	41.41	-0.23	336	(Davis and Stevenson, 2007)
Laguna Guallar	N-GUA_micro	41.41	-0.23	336	(Davis and Stevenson, 2007)
Lake Banyoles	Banyoles SB2	42.13	2.75	174	(Revelles et al., 2015)
Lanzahita	Lanzahita core	40.22	-4.94	588	(López-Sáez et al., 2018b)
Las Animas Mire	Las Animas Mire core_macro	36.69	-5.03	1403	(Alba-Sánchez et al., 2019)
Las Animas Mire	Las Animas Mire core_micro	36.69	-5.03	1403	(Alba-Sánchez et al., 2019)
Las Pardillas	Las Pardillas core	42.03	-3.03	1850	(Sanchez Goñi and Hannon, 1999)
Las Vinuelas	Las Vinuelas core_macro	39.37	-4.49	761	(Morales - Molino et al., 2019)
Las Vinuelas	Las Vinuelas core_micro	39.37	-4.49	761	(Morales - Molino et al., 2019)
Manaderos	Manaderos core	40.34	-4.69	1292	(Robles-López et al., 2020)
Marbore	Marbore composite	42.70	0.04	2612	(Leunda et al., 2017)
Navamuno	Navamuno_S3	40.32	-5.78	1505	(Turu et al., 2018; López-Sáez et al., 2020)
Navarres	NAVARRE3	39.10	-0.68	225	(Carrión and Van Geel, 1999)
Ojos del Tremendal	Ojos del Tremendal core	40.54	-2.05	1650	(Stevenson, 2000)
Pena da Cadela	Pena da Cadela core	42.83	-7.17	970	(Martínez Cortizas et al., 2002)
Pena Negra	Pena Negra core	40.33	-5.79	1000	(Abel-Schaad and López-Sáez, 2013)
Pozo de la Nieve	PozoN_2015 core	40.35	-4.55	1600	(Robles-López et al., 2017)
Puerto de Serranillos	Serranillos_macro	40.31	-4.93	1700	(López-Sáez et al., 2018b)
Puerto de Serranillos	Serranillos_micro	40.31	-4.93	1700	(López-Sáez et al., 2018b)

Puerto del Pico	Puerto del Pico core_macro	40.32	-5.01	1395	(López-Sáez et al., 2016a)
Puerto del Pico	Puerto del Pico core_micro	40.32	-5.01	1395	(López-Sáez et al., 2016a)
Sierra de Gador	Gador core	36.90	-2.92	1530	(Carrión et al., 2003)
Siles Lake	Siles Lake core	38.40	-2.50	1320	(Carrión, 2002)
Tubilla del Lago	Tubilla del Lago core	41.81	-3.57	900	(Morales-Molino et al., 2017b)
Valle do Lobo Ribeira de Carcavai	VdL PB2_100minus	37.06	-8.07	2.3	(Schneider et al., 2010, 2016)
Valle do Lobo Ribeira de Carcavai	VdL PB2_100plus	37.06	-8.07	2.3	(Schneider et al., 2010, 2016)
Verdeospesoa	Verdeospesoa core	43.06	-2.86	1015	(Pérez-Díaz and López-Sáez, 2017, 2019)
Vilamora Ribeira de Quarteira	Vilamora P01-5_100minus	37.09	-8.14	3.5	(Schneider et al., 2010, 2016)
Vilamora Ribeira de Quarteira	Vilamora P01-5_100plus	37.09	-8.14	3.5	(Schneider et al., 2010, 2016)
Villaverde	Villaverde core	38.80	-2.37	870	(Carrión et al., 2001b)

#### S4. Selection of the final GLM

We initially examined 13 variables that have been shown in global analyses to influence burnt area. Table S5 provides information on the source of each of the data sets, their original resolution, and the transformation used prior to analysis.

70 **Table S5.** Environmental variables and transformation methods.

Environmental variables	Data source	Resolution	Transformation	Reference
Dry days per month	CRUNCEP V7	$0.5^\circ \times 0.5^\circ$	Logarithmic	Viovy, 2018
Diurnal temperature range (K)	CRUNCEP V7	$0.5^\circ \times 0.5^\circ$	Logarithmic	Viovy, 2018
Maximum temperature (K)	CRUNCEP V7	$0.5^\circ \times 0.5^\circ$	Logarithmic	Viovy, 2018
Wind speed (m/s)	CRUNCEP V7	$0.5^\circ \times 0.5^\circ$	Logarithmic	Viovy, 2018
Gross primary production ( $\text{gC m}^{-2} \text{ day}^{-1}$ )	FLUXCOM	$0.5^\circ \times 0.5^\circ$	Logarithmic	Jung et al., 2020
Tree cover (%)	VCF	$0.05^\circ \times 0.05^\circ$	Cell fraction	Hansen and Song, 2018
Non-tree cover (%)	VCF	$0.05^\circ \times 0.05^\circ$	Cell fraction	Hansen and Song, 2018
Cropland ( $\text{km}^2$ )	HYDE 3.2	$0.083^\circ \times 0.083^\circ$	Cell fraction	Klein Goldewijk et al., 2017
Total rainfed other crops (no rice) ( $\text{km}^2$ )	HYDE 3.3	$0.083^\circ \times 0.083^\circ$	Cell fraction	Klein Goldewijk et al., 2017
Grazing land ( $\text{km}^2$ )	HYDE 3.2	$0.083^\circ \times 0.083^\circ$	Cell fraction	Klein Goldewijk et al., 2017
Total population density (inhabitants $\text{km}^{-2}$ )	HYDE 3.2	$0.083^\circ \times 0.083^\circ$	Square root	Klein Goldewijk et al., 2017
Urban population density (inhabitants $\text{km}^{-2}$ )	HYDE 3.2	$0.083^\circ \times 0.083^\circ$	Square root	Klein Goldewijk et al., 2017
Rural population density (inhabitants $\text{km}^{-2}$ )	HYDE 3.2	$0.083^\circ \times 0.083^\circ$	Square root	Klein Goldewijk et al., 2017

**The process of final model selection:** The partial correlation test (Fig. S1) shows that tree cover is highly correlated with both GPP (0.63) and non-tree cover (0.69), and rainfed cropland is highly correlated with total cropland (0.62). The three population variables are also strongly correlated with one another ( $> 0.80$ ). There are moderate correlations between maximum

75 temperature of the warmest month, maximum diurnal temperature range, and maximum dry days per month ( $> 0.40$ ). We tested the impact of including or removing highly and moderately correlated variables before selecting the final model. Tree cover was not included in any GLM model because of its high correlation with both GPP and non-tree cover. The GLM model including cropland has a higher pseudo- $R^2$  than the model including total rainfed cropland (Table S6: first 2 columns), so only total cropland was retained. Comparison of the GLM models using total, urban and rural population density (Table S6: 2-4 columns) shows that only urban population density is statistically significant and the model with urban population density has the best fit (pseudo- $R^2=0.20$ ). All the variables in this model, except for maximum temperature, are statistically significant ( $P < 0.1$ ). Given the lack of statistical significance of maximum temperature and the moderate correlations between maximum

temperature and both diurnal temperature range and dry days per month (Fig. S1), we constructed three models leaving out one variable in turn. We obtained pseudo- $R^2$  values of 0.20, 0.17 and 0.20 respectively for these three models (Table S6: the last 3 columns). The model which does not include maximum temperature has the best fit (pseudo- $R^2=0.20$ ). The final model was constructed using eight variables (Table S6: the last column).

**Figure S1.** Partial correlations test based on data sets for the Iberian Peninsula that include annual observations at 0.5° for the period between 2001 and 2016. The data are all transformed according to Table S5 prior to the test.

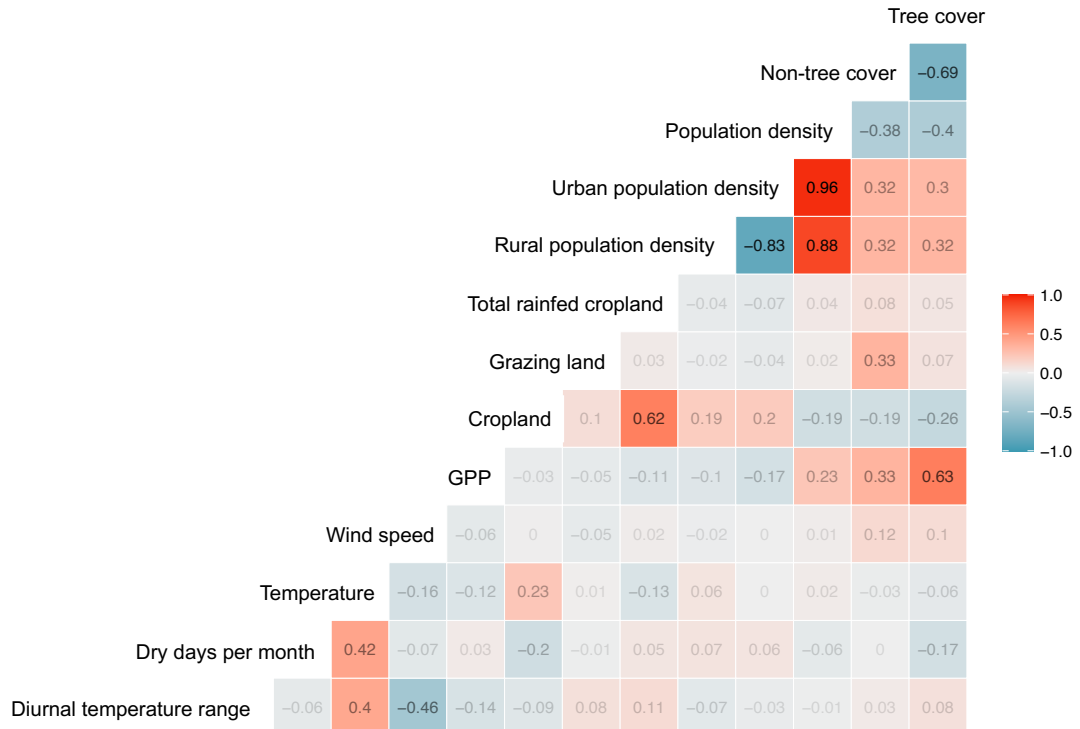


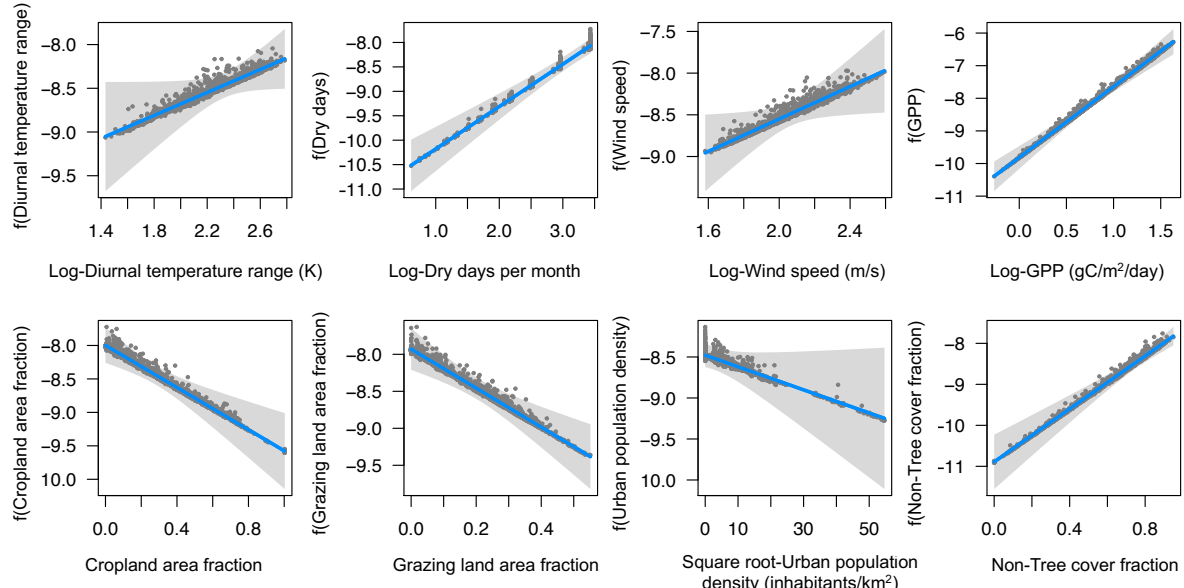
**Table S6.** The process of the model selection. Regression coefficients (t value) and pseudo-R<sup>2</sup> of each model are shown. The final model is shown in bold.

	1 Include total rainfed cropland	2 Include total population density	3 Include rural population density	4 Include urban population density	5 Remove diurnal temperature range	6 Remove dry days per month	7 <b>Remove maximum temperature</b>
Diurnal temperature range	1.95	1.86	2.38*	1.77		1.19	<b>1.90</b>
Dry days per month	7.81***	7.66***	7.56***	7.66***	-1.01***		<b>8.46***</b>
Maximum temperature	-0.50	0.01	-0.19	0.07	7.60	4.07***	
Wind speed	2.00*	2.04*	2.05*	2.07*	0.69	1.89	<b>2.11*</b>
GPP	9.54***	9.76***	9.49***	9.85***	1.43***	9.41***	<b>10.10***</b>
Non-tree cover	7.11***	7.27***	7.19***	7.33***	7.44***	9.50***	<b>7.34***</b>
Cropland		-3.95***	-4.08***	-3.95***	9.76***	-4.86***	<b>-4.04***</b>
Total rainfed cropland	-3.62***						
Grazing land	-4.64***	-4.29***	-4.19***	-4.36***	-4.17***	-4.96***	<b>-4.36***</b>
Total population density	-1.55	-1.07					
Rural population density			0.06				
Urban population density				-1.68	-2.32*	-1.38	<b>-1.69</b>
Pseudo-R <sup>2</sup>	0.2008	0.2031	0.2013	0.2020	0.2012	0.1654	<b>0.2031</b>

95 Notes: ·p < 0.1; \*p < 0.05; \*\*p < 0.01; \*\*\*p < 0.001.

Figure S2 shows the partial residuals obtained for the final model.

**Figure S2.** Partial residual plots of the final model (Table S6, last column). The plot includes (1) the expected value (blue line); (2) a confidence interval for the expected value (grey band); (3) partial residuals (dark grey dots)



100

## S5. Box-Cox transformation of palaeo burnt area fraction

The standard Box-Cox transformation is:

$$Y_i^{(\lambda)} = \begin{cases} \frac{Y_i^{(\lambda)} - 1}{\lambda} & (\lambda \neq 0) \\ \log(Y_i) & (\lambda = 0) \end{cases}$$

105 The inverse Box-Cox transformation is:

$$Y_i = \begin{cases} \exp\left(\frac{\log(1 + \lambda Y_i^{(\lambda)})}{\lambda}\right) & (\lambda \neq 0) \\ \exp(Y_i^{(\lambda)}) & (\lambda = 0) \end{cases}$$

After deriving palaeo burnt area fraction from charcoal by applying conversion factors, we applied the Box-Cox transformation to the palaeo burnt area fraction to reduce the skewness of the data. The parameter  $\lambda$  was set as 0.25 after trials of a range of 110 values (Figure S3, Table S7). This value has the highest predictive power ( $R^2 = 0.436$ ) and less local compression ( $b_1 = 0.526$ ) compared to using other values of  $\lambda$ . Figure S3 shows the change in the distribution of palaeo burnt area fraction before and

after Box-Cox transformation. The predicted values of palaeo burnt area fraction from fxTWAPLS were then obtained via the inverse Box-Cox transformation.

115

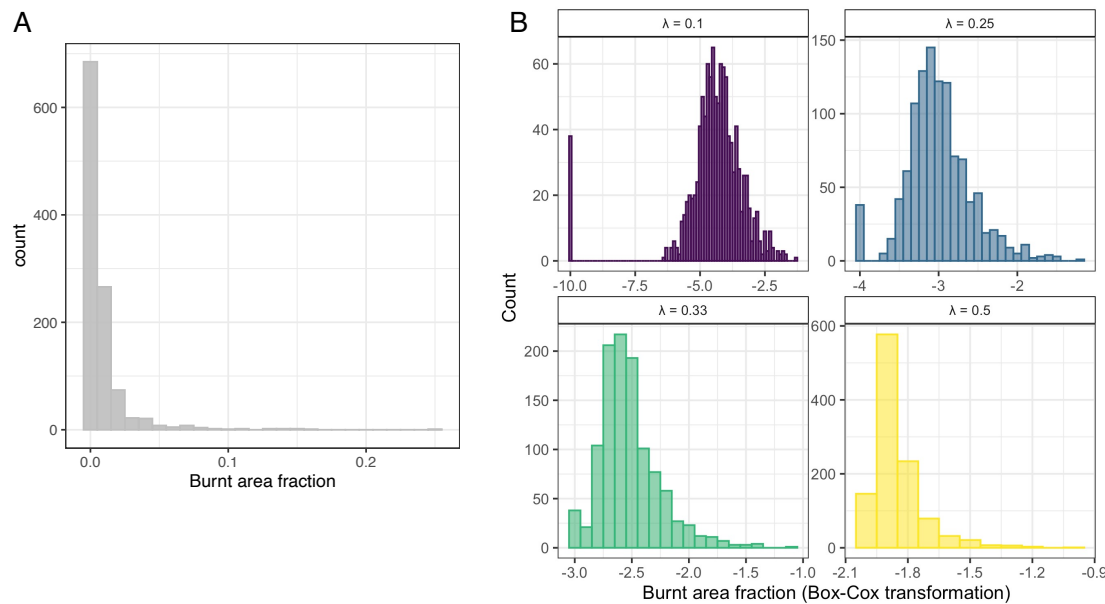


**Figure S3.** Distribution of palaeo burnt area fraction before (Panel A) and after (Panel B) Box-Cox transformation.

120 **Table S7.** Results of fxTWAPLS using different values of  $\lambda$ .

method	ncomp	R <sup>2</sup>	RMSEP	ΔRMSEP	p	b <sub>0</sub>	b <sub>1</sub>	b <sub>0</sub> .se	b <sub>1</sub> .se
$\lambda = 0.1$	1	0.227	1.184	-9.799	0.001	-3.453	0.175	0.045	0.010
	2	0.289	1.135	-4.126	0.001	-3.283	0.220	0.048	0.010
	3	0.380	1.042	-8.182	0.001	-2.669	0.371	0.066	0.014
	4	0.399	1.026	-1.531	0.010	-2.460	0.420	0.072	0.016
	5	0.416	1.011	-1.490	0.002	-2.452	0.421	0.070	0.015
	<b>6</b>	<b>0.425</b>	<b>1.002</b>	<b>-0.882</b>	<b>0.002</b>	<b>-2.456</b>	<b>0.423</b>	<b>0.069</b>	<b>0.015</b>
	7	0.429	1.004	0.161	0.560	-2.531	0.400	0.064	0.014
	8	0.427	1.007	0.327	0.761	-2.529	0.398	0.064	0.014
$\lambda = 0.25$	1	0.249	0.366	-11.172	0.001	-2.083	0.280	0.044	0.015
	2	0.333	0.340	-7.027	0.001	-1.822	0.380	0.049	0.016
	3	0.404	0.326	-4.332	0.005	-1.467	0.502	0.056	0.018
	<b>4</b>	<b>0.436</b>	<b>0.316</b>	<b>-2.988</b>	<b>0.012</b>	<b>-1.390</b>	<b>0.526</b>	<b>0.054</b>	<b>0.018</b>
	5	0.439	0.316	-0.006	0.483	-1.381	0.526	0.054	0.018
	6	0.443	0.313	-0.857	0.230	-1.402	0.520	0.053	0.018
	7	0.461	0.308	-1.584	0.010	-1.343	0.541	0.053	0.018
	8	0.474	0.305	-0.909	0.081	-1.282	0.561	0.054	0.018

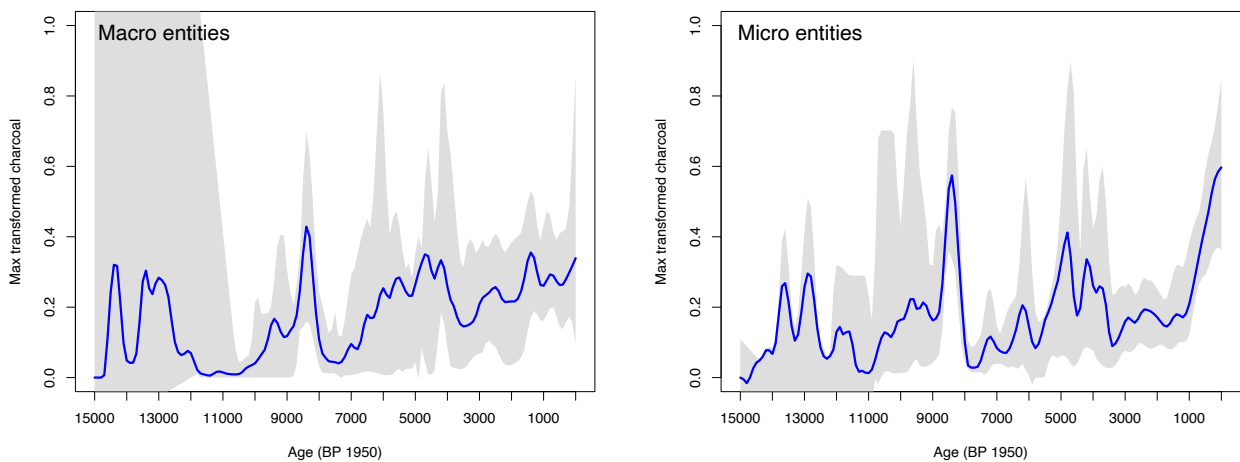
	1	0.240	0.240	-10.025	0.001	-1.708	0.304	0.041	0.016
	2	0.326	0.223	-7.049	0.001	-1.492	0.399	0.044	0.017
	3	0.400	0.213	-4.610	0.005	-1.209	0.514	0.048	0.019
$\lambda = 0.33$	<b>4</b>	<b>0.431</b>	<b>0.208</b>	<b>-2.541</b>	<b>0.039</b>	<b>-1.143</b>	<b>0.537</b>	<b>0.047</b>	<b>0.019</b>
	5	0.421	0.212	2.251	0.952	-1.109	0.548	0.049	0.019
	6	0.436	0.207	-2.263	0.001	-1.113	0.548	0.048	0.019
	7	0.447	0.206	-0.641	0.193	-1.054	0.574	0.049	0.019
	8	0.451	0.205	-0.736	0.176	-1.073	0.564	0.048	0.019
	<b>1</b>	<b>0.209</b>	<b>0.120</b>	<b>-0.030</b>	<b>0.500</b>	<b>-1.285</b>	<b>0.279</b>	<b>0.030</b>	<b>0.016</b>
	2	0.293	0.109	-8.666	0.001	-1.177	0.343	0.030	0.016
	3	0.361	0.103	-6.261	0.001	-0.953	0.470	0.035	0.019
$\lambda = 0.5$	4	0.384	0.102	-0.892	0.242	-0.917	0.488	0.035	0.019
	5	0.375	0.103	1.681	0.954	-0.868	0.515	0.037	0.020
	6	0.396	0.101	-2.624	0.001	-0.856	0.522	0.036	0.019
	7	0.396	0.100	-0.312	0.341	-0.824	0.542	0.037	0.020
	8	0.401	0.100	-0.644	0.241	-0.826	0.541	0.037	0.020

## S6. Impact of using of micro and macro charcoal on the burnt area fraction reconstructions

The charcoal data used in these analyses was generated in several different ways and includes counts of both microcharcoal and macrocharcoal. Some sites had only macroscopic charcoal, some only microscopic charcoal, and a small number of sites included both. Macrocharcoal is often thought to be associated with local fires, and microcharcoal to represent regional fires.

- 125 In order to test whether size had any impact of the composite reconstructions, we compared the 16 charcoal sites with both macroscopic and microscopic records (Fig. S4). Since this analysis suggests there is no difference in the curves obtained, we used both types of record in our analyses, though preferring macrocharcoal at those sites with both kinds of records.

130 **Figure S4.** Composite plots for macroscopic and macroscopic charcoal separately of 16 charcoal sites with both macroscopic and microscopic entities using the locfit() function with half-width=300, number of bootstrap samples=1000. The locally estimated scatterplot smoothing is shown in blue; The upper and lower 95th-percentile confidence intervals are shown in grey.



## S7. Comparisons of WA-PLS and TWA-PLS reconstructions with and without fx correction

Weighted Averaging Partial Least-Squares (WA-PLS) regression (ter Braak et al., 1993; ter Braak and Juggins, 1993; Salonen et al., 2012) is widely used for climate reconstructions, but there is a known tendency for the reconstructed values to be compressed towards the middle of the range of the climate variable as expressed in the training data set.

135 Tolerance-weighted Weighted Averaging Partial Least-Squares with a sampling frequency correction (fxTWA-PLS: Liu et al., 2020) is a modification of WA-PLS, designed to reduce the compression of reconstructions towards the centre of the climatic range sampled by the training dataset by accounting for the climatic tolerances of individual pollen taxa and the frequency (fx) of the sampled climate variable in the training dataset. Since fxTWA-PLS has not previously been used to reconstruct burnt area fractions, we tested whether this approach reduced compression in the burnt area fraction reconstructions when compared to WA-PLS. We also tested the impact of using the sampling frequency correction (fx) separately for both WA-PLS and TWA-PLS. Cross-validation fitness assessment (Table S8) and visual comparison of the fitted plots and residuals (Fig. S5) indicate that fxTWA-PLS reduces the compression bias more than other methods and also has higher predictive power. The composite 140 curves produced using each approach are shown in Fig. S6.

**Table S8.** Leave-out cross-validation fitness of WA-PLS and TWA-PLS methods, with and without fx correction, showing results for all the components. The last significant number of components are shown in bold.

method	ncomp	R <sup>2</sup>	RMSEP	ΔRMSEP	p	b0	b1	b0.se	b1.se
WA-PLS	1	0.260	0.355	-13.870	0.001	-2.190	0.274	0.042	0.014
	2	0.341	0.336	-5.487	0.001	-1.906	0.370	0.047	0.015
	3	0.390	0.322	-3.936	0.001	-1.785	0.409	0.047	0.015
	<b>4</b>	<b>0.405</b>	<b>0.318</b>	<b>-1.196</b>	<b>0.003</b>	<b>-1.738</b>	<b>0.424</b>	<b>0.047</b>	<b>0.015</b>
	5	0.418	0.315	-0.961	0.163	-1.659	0.451	0.048	0.016
	6	0.425	0.314	-0.576	0.226	-1.629	0.461	0.049	0.016
	7	0.427	0.313	-0.239	0.391	-1.623	0.462	0.049	0.016
	8	0.432	0.312	-0.210	0.400	-1.584	0.476	0.050	0.016
TWA-PLS	1	0.249	0.357	-13.313	0.001	-2.285	0.239	0.038	0.013
	2	0.334	0.337	-5.624	0.001	-1.950	0.355	0.046	0.015
	3	0.403	0.319	-5.349	0.001	-1.732	0.427	0.047	0.016
	4	0.434	0.311	-2.658	0.001	-1.637	0.459	0.048	0.016
	<b>5</b>	<b>0.450</b>	<b>0.306</b>	<b>-1.476</b>	<b>0.019</b>	<b>-1.589</b>	<b>0.474</b>	<b>0.048</b>	<b>0.016</b>
	6	0.462	0.303	-1.034	0.074	-1.557	0.484	0.048	0.016
	7	0.465	0.302	-0.207	0.380	-1.532	0.493	0.048	0.016
	8	0.473	0.300	-0.771	0.120	-1.494	0.505	0.049	0.016
WA-PLS with fx correction	1	0.260	0.363	-12.037	0.001	-2.038	0.297	0.046	0.015
	<b>2</b>	<b>0.339</b>	<b>0.343</b>	<b>-5.337</b>	<b>0.001</b>	<b>-1.660</b>	<b>0.438</b>	<b>0.056</b>	<b>0.018</b>
	3	0.373	0.333	-3.100	0.099	-1.612	0.450	0.053	0.018
	4	0.392	0.329	-1.028	0.120	-1.506	0.486	0.055	0.018
	5	0.410	0.326	-1.077	0.151	-1.424	0.513	0.056	0.019
	6	0.416	0.323	-0.822	0.256	-1.421	0.515	0.056	0.018
	7	0.399	0.329	1.972	0.937	-1.453	0.501	0.056	0.018
	8	0.405	0.327	-0.553	0.005	-1.438	0.506	0.056	0.018
TWA-PLS with fx correction	1	0.249	0.366	-11.172	0.001	-2.083	0.280	0.044	0.015
	2	0.333	0.340	-7.027	0.001	-1.822	0.380	0.049	0.016
	3	0.404	0.326	-4.332	0.005	-1.467	0.502	0.056	0.018
	<b>4</b>	<b>0.436</b>	<b>0.316</b>	<b>-2.988</b>	<b>0.012</b>	<b>-1.390</b>	<b>0.526</b>	<b>0.054</b>	<b>0.018</b>
	5	0.439	0.316	-0.006	0.483	-1.381	0.526	0.054	0.018
	6	0.443	0.313	-0.857	0.230	-1.402	0.520	0.053	0.018
	7	0.461	0.308	-1.584	0.010	-1.343	0.541	0.053	0.018
	8	0.474	0.305	-0.909	0.081	-1.282	0.561	0.054	0.018

155 **Figure S5.** The fitted plots and residual plots of WA-PLS and TWA-PLS methods, with and without fx correction.

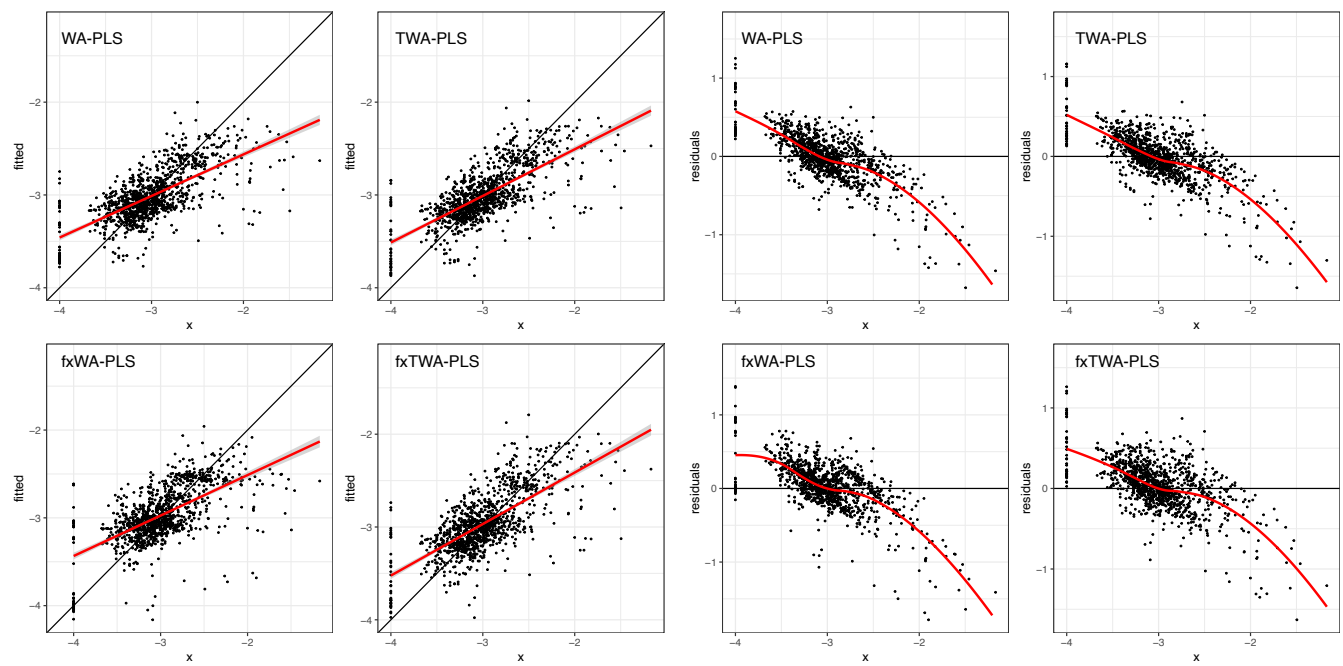
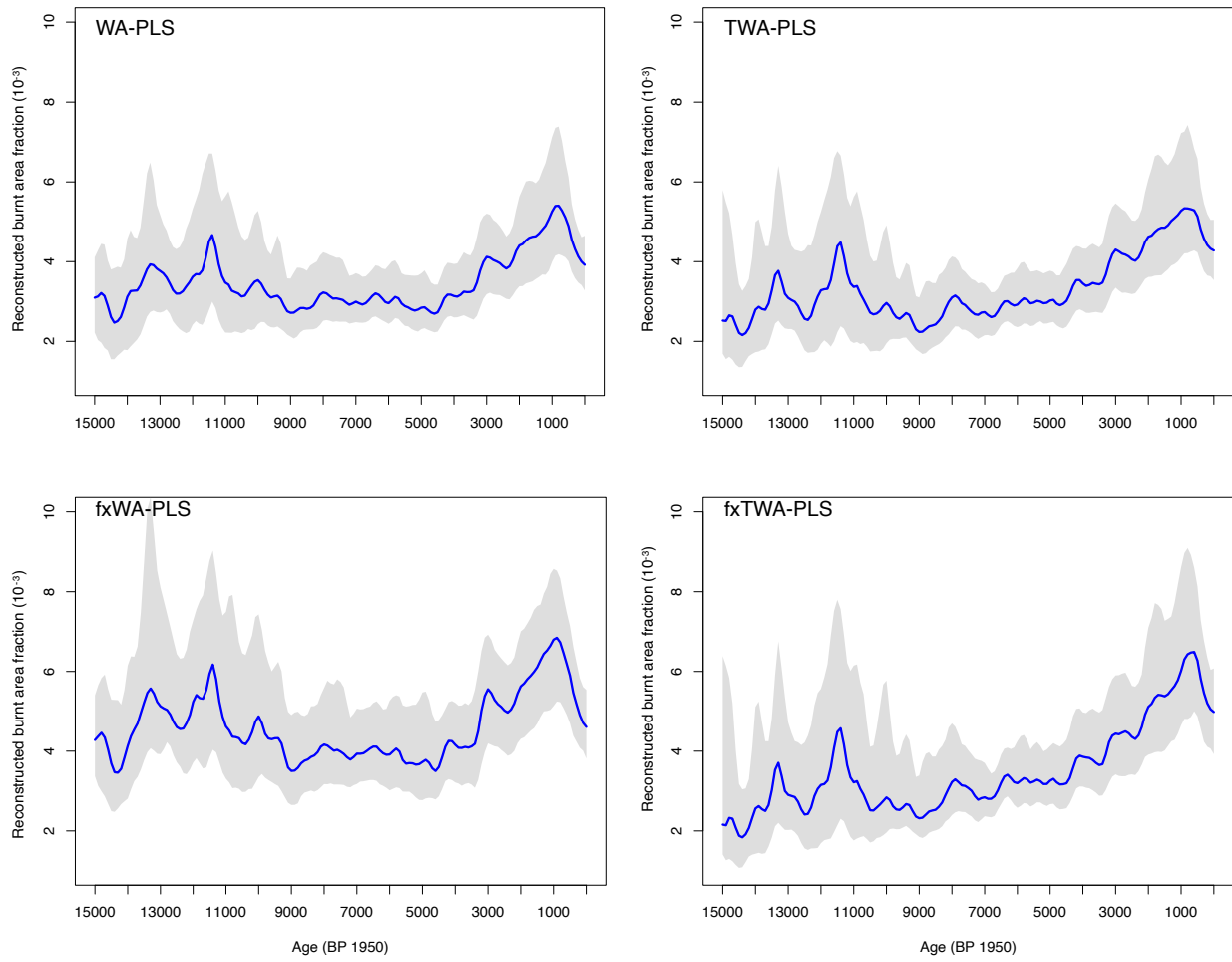


**Figure S6.** Composite curves of reconstructed burnt area using WA-PLS and TWA-PLS, with and without fx correction, using the locfit() function with half-width = 300, number of bootstrap samples = 1000. The locally estimated scatterplot smoothing 160 is shown in blue; The upper and lower 95th-percentile confidence intervals are shown in grey.



## References

- Abel-Schaad, D. and López-Sáez, J. A.: Vegetation changes in relation to fire history and human activities at the Peña Negra mire (Bejar Range, Iberian Central Mountain System, Spain) during the past 4,000 years, *Veg. Hist. Archaeobot.*, 22(3), 165 199–214, doi:10.1007/s00334-012-0368-9, 2013.
- Abel-Schaad, D., Alba-Sánchez, F., Pérez-Díaz, S. and López-Sáez, J. A.: 36. Prailllos de Boissier mire, Tejeda Natural Park (Baetic Range, southern Spain), *Grana*, 56(6), 475–477, doi:10.1080/00173134.2017.1282977, 2017.
- Abel-Schaad, D., Hernández Carretero, A. M., López-Merino, L., Pulido Díaz, F. J. and López Sáez, J. A.: Cabras y quemorros: tres siglos de cambios en el paisaje de la vertiente extremeña de la Sierra de Gredos, *Rev. Estud. Extremenos*, 1, 170 449–478, 2009a.
- Abel-Schaad, D., Hernández, A., López Sáez, J. A., Pulido Díaz, F. J., López Merino, L. and Martínez Cortizas, A.: Evolución de la vegetación en la Sierra de Gata (Cáceres-Salamanca, España) durante el Holoceno reciente. Implicaciones biogeográficas, *Rev. Española Micropaleontol.*, 41(1–2), 91–105, 2009b.
- Alba-Sánchez, F., López-Sáez, J. A., Abel-Schaad, D., Sabariego Ruiz, S., Pérez-Díaz, S., González-Hernández, A. and 175 Linares, J. C.: The impact of climate and land-use changes on the most southerly fir forests (*Abies pinsapo*) in Europe, *The Holocene*, 29(7), 1176–1188, doi:10.1177/0959683619838043, 2019.
- Allen, J. R. M., Huntley, B. and Watts, W. A.: The vegetation and climate of northwest Iberia over the last 14,000 years, *J. Quat. Sci.*, 11(2), 125–147, doi:10.1002/(SICI)1099-1417(199603/04)11:2<125::AID-JQS232>3.0.CO;2-U, 1996.
- Anderson, R. S., Jiménez-Moreno, G., Carrión, J. S. and Pérez-Martínez, C.: Postglacial history of alpine vegetation, fire, 180 and climate from Laguna de Río Seco, Sierra Nevada, southern Spain, *Quat. Sci. Rev.*, 30(13–14), 1615–1629, doi:10.1016/j.quascirev.2011.03.005, 2011.
- De Beaulieu, J.-L., Miras, Y., Andrieu-Ponel, V. and Guiter, F.: Vegetation dynamics in north-western Mediterranean regions: instability of the Mediterranean bioclimate, *Plant Biosyst. Int. J. Deal. with all Asp. Plant Biol.*, 139(2), 114–126, 2005.
- ter Braak, C. J. F. and Juggins, S.: Weighted averaging partial least squares regression (WA-PLS): an improved method for 185 reconstructing environmental variables from species assemblages, *Hydrobiologia*, 269–270(1), 485–502, doi:10.1007/BF00028046, 1993.
- ter Braak, C. J. F., Juggins, S., Birks, H. J. B. and van der Voet, H.: Weighted averaging partial least squares regression (WA-PLS): Definition and comparison with other methods for species-environment calibration, in *Multivariate 190 Environmental statistics*, edited by G. P. Patil and C. R. Rao, pp. 525–560, Elsevier, Amsterdam. [online] Available from: <https://edepot.wur.nl/249353>, 1993.

Van Den Brink, L. M. and Janssen, C. R.: The effect of human activities during cultural phases on the development of montane vegetation in the Serra de Estrela, Portugal, *Rev. Palaeobot. Palynol.*, 44(3–4), 193–215, doi:10.1016/0034-6667(85)90016-8, 1985.

- 195 Burjachs, F.: Palynology of the Upper Pleistocene and Holocene of the North-East Iberian Peninsula: Pla De L'estany (Catalonia), *Hist. Biol.*, 9(1–2), 17–33, doi:10.1080/10292389409380485, 1994.

Burjachs, F., Giralt, S., Roca, J. R., Seret, G., Julia, R. and Ediciones, G.: Palinologia holocenica y desertizacion en el mediterraneo occidental, in *El paisaje mediterraneo a traves del espacio y del tiempo. Implicaciones en la desertizacion.*, edited by J. J. Ibáñez, B. L. Valero Garcés, and C. Machado, pp. 379–394, Geoforma, Logroño., 1997

- 200 Burjachs, F.: La secuencia palinológica de La Cruz (Cuenca, España), in *Estudios palinológicos*, edited by M. B. Ruz-Zapata, pp. 31–36, Servicio de Publicaciones de la Universidad de Alcalá edition, Spain., 1996.

Burjachs, F. and Expósito, I.: Charcoal and pollen analysis: Examples of Holocene fire dynamics in Mediterranean Iberian Peninsula, *Catena*, 135, 340–349, doi:10.1016/j.catena.2014.10.006, 2015.

- 205 Burjachs, F., Pérez-Obiol, R., Picornell-Gelabert, L., Revelles, J., Servera-Vives, G., Expósito, I. and Yll, E. I.: Overview of environmental changes and human colonization in the Balearic Islands (Western Mediterranean) and their impacts on vegetation composition during the Holocene, *J. Archaeol. Sci. Reports*, 12, 845–859, doi:10.1016/j.jasrep.2016.09.018, 2017.

Cano Villanueva, J. P.: Estudi palinologic de sediments litorals de la província d'Almeria. Transformacions del paisatge vegetal en un territori semiarid, Universitat Autònoma de Barcelona, Barcelona, Spain. [online] Available from:

- 210 <https://dialnet.unirioja.es/servlet/tesis?codigo=247794&info=resumen&idioma=SPA> (Accessed 22 March 2021), 1997.

Carrión, J. S. and Dupré, M.: Late Quaternary vegetational history at Navarrés, Eastern Spain. A two core approach, *New Phytol.*, 134(1), 177–191, doi:10.1111/j.1469-8137.1996.tb01157.x, 1996.

Carrión, J. S., Munuera, M., Dupré, M. and Andrade, A.: Abrupt vegetation changes in the Segura Mountains of southern Spain throughout the Holocene, *J. Ecol.*, 89(5), 783–797, 2001.

- 215 Carrión, J. S.: Patterns and processes of Late Quaternary environmental change in a montane region of southwestern Europe, *Quat. Sci. Rev.*, 21(18–19), 2047–2066, doi:10.1016/S0277-3791(02)00010-0, 2002.

Carrión, J. S. and Van Geel, B.: Fine-resolution Upper Weichselian and Holocene palynological record from Navarrés (Valencia, Spain) and a discussion about factors of Mediterranean forest succession, *Rev. Palaeobot. Palynol.*, 106(3–4), 209–236, doi:10.1016/S0034-6667(99)00009-3, 1999.

- 220 Carrión, J. S., Munuera, M., Dupré, M. and Andrade, A.: Abrupt vegetation changes in the Segura Mountains of southern Spain throughout the Holocene, *J. Ecol.*, 89(5), 783–797, doi:10.1046/j.0022-0477.2001.00601.x, 2001a.

Carrión, J. S., Andrade, A., Bennett, K. D., Navarro, C. and Munuera, M.: Crossing forest thresholds: inertia and collapse in a Holocene sequence from south-central Spain, *The Holocene*, 11(6), 635–653, doi:10.1191/09596830195672, 2001b.

Carrión, J. S., Sánchez-Gómez, P., Mota, J. F., Yll, R. and Chaín, C.: Holocene vegetation dynamics, fire and grazing in the  
225 Sierra de Gádor, southern Spain, *The Holocene*, 13(6), 839–849, doi:10.1191/0959683603hl662rp, 2003.

Carrión, J. S., Yll, E. I., Willis, K. J. and Sánchez, P.: Holocene forest history of the eastern plateaux in the Segura Mountains (Murcia, southeastern Spain), *Rev. Palaeobot. Palynol.*, 132(3–4), 219–236, doi:10.1016/j.revpalbo.2004.07.002, 2004.

Carrión, J. S., Fuentes, N., González-Sampériz, P., Sánchez Quirante, L., Finlayson, J. C., Fernández, S. and Andrade, A.:  
230 Holocene environmental change in a montane region of southern Europe with a long history of human settlement, *Quat. Sci. Rev.*, 26(11–12), 1455–1475, doi:10.1016/j.quascirev.2007.03.013, 2007.

Cerrillo Cuenca, E. and González Cordero, A.: Burial prehistoric caves in the interior basin of River Tagus: the complex at Canaleja Gorge (Romangordo, Cáceres, Spain), *BAR Int. Ser.*, 2219, 21–42, 2011.

Cerrillo Cuenca, E., González Cordero, A. and López Sáez, J. A.: El proyecto de investigación de Garganta Canaleja:  
235 aproximación al análisis del Epipaleolítico y el Neolítico en el valle interior del Tajo, Los Prim. Campesinos la Raya. Actas las jornadas Arqueol. del Mus. Cáceres., 13–27, 2007.

Connor, S. E., Araújo, J., van der Knaap, W. O. and van Leeuwen, J. F. N.: A long-term perspective on biomass burning in the Serra da Estrela, Portugal, *Quat. Sci. Rev.*, 55, 114–124, doi:10.1016/j.quascirev.2012.08.007, 2012.

Cortés-Sánchez, M., Morales-Muñiz, A., Simón-Vallejo, M. D., Bergadà-Zapata, M. M., Delgado-Huertas, A., López-  
240 García, P., López-Sáez, J. A., Lozano-Francisco, M. C., Riquelme-Cantal, J. A. and Roselló-Izquierdo, E.: Palaeoenvironmental and cultural dynamics of the coast of Málaga (Andalusia, Spain) during the Upper Pleistocene and early Holocene, *Quat. Sci. Rev.*, 27(23–24), 2176–2193, 2008.

Cortés-Sánchez, M., Morales-Muñiz, A., Simón-Vallejo, M. D., Lozano-Francisco, M. C., Vera-Peláez, J. L., Finlayson, C., Rodríguez-Vidal, J., Delgado-Huertas, A., Jiménez-Espejo, F. J. and Martínez-Ruiz, F.: Earliest known use of marine  
245 resources by Neanderthals, *PLoS One*, 6(9), e24026, 2011.

Davis, B. and Stevenson, A.: The 8.2ka event and Early–Mid Holocene forests, fires and flooding in the Central Ebro Desert, NE Spain, *Quat. Sci. Rev.*, 26(13–14), 1695–1712, doi:10.1016/j.quascirev.2007.04.007, 2007.

Davis, B. A. S.: Pollen profile N-PEQ, Salada Pequeña, Spain, Eur. Pollen Database (EPD), PANGAEA,  
doi:<https://doi.org/10.1594/PANGAEA.738850>, 2010.

250 Dorado-Valiño, M., López-Sáez, J. A. and García-Gómez, E.: 21. Patateros, Toledo Mountains (central Spain), *Grana*, 53(2), 171–173, doi:10.1080/00173134.2014.903293, 2014.

Ejarque, A., Julià, R., Reed, J. M., Mesquita-Joanes, F., Marco-Barba, J. and Riera, S.: Coastal Evolution in a Mediterranean Microtidal Zone: Mid to Late Holocene Natural Dynamics and Human Management of the Castelló Lagoon, NE Spain, edited by J. M. Dias, PLoS One, 11(5), e0155446, doi:10.1371/journal.pone.0155446, 2016.

255 Engelbrechten, S. Von: Late-glacial and holocene vegetation and environmental history of the Sierra de Urbión, North-West Central Spain, Trinity College, Dublin, Ireland., 1999.

Franco-Múgica, F., García-Antón, M., Maldonado-Ruiz, J., Morla-Juaristi, C. and Sainz-Ollero, H.: Ancient pine forest on inland dunes in the Spanish northern meseta, *Quat. Res.*, 63(1), 1–14, doi:10.1016/j.yqres.2004.08.004, 2005.

260 Garces-Pastor, S., Canellas-Bolta, N., Clavaguera, A., Calero, M. A. and Vegas-Vilarrubia, T.: Vegetation shifts, human impact and peat bog development in Bassa Nera pond (Central Pyrenees) during the last millennium, *The Holocene*, 27(4), 553–565, 2017.

Gil-Romera, G., García Antón, M. and Calleja, J. A.: The late Holocene palaeoecological sequence of Serranía de las Villuercas (southern Meseta, western Spain), *Veg. Hist. Archaeobot.*, 17(6), 653–666, doi:10.1007/s00334-008-0146-x, 2008.

265 Gomes, S. D.: 13. Lake Saloio (Nazaré, western Portugal), *Grana*, 50(3), 228–231, doi:10.1080/00173134.2011.579620, 2011.

González-Ramón, A., Andreo, B., Ruiz-Bustos, A., Richards, D. A., López-Sáez, J. A. and Alba-Sánchez, F.: Late Quaternary paleoenvironmental record from a sedimentary fill in Cucú cave, Almería, SE Spain, *Quat. Res.*, 77(2), 264–272, 2012.

270 González-Sampériz, P., Valero-Garcés, B. L., Moreno, A., Jalut, G., García-Ruiz, J. M., Martí-Bono, C., Delgado-Huertas, A., Navas, A., Otto, T. and Dedoubat, J. J.: Climate variability in the Spanish Pyrenees during the last 30,000 yr revealed by the El Portalet sequence, *Quat. Res.*, 66(1), 38–52, doi:10.1016/j.yqres.2006.02.004, 2006.

275 González-Sampériz, P., Aranbarri, J., Pérez-Sanz, A., Gil-Romera, G., Moreno, A., Leunda, M., Sevilla-Callejo, M., Corella, J. P., Morellón, M., Oliva, B. and Valero-Garcés, B.: Environmental and climate change in the southern Central Pyrenees since the Last Glacial Maximum: A view from the lake records, *Catena*, 149, 668–688, doi:10.1016/j.catena.2016.07.041, 2017.

280 González-Sampériz, P., Gil-Romera, G., García-Prieto, E., Aranbarri, J., Moreno, A., Morellón, M., Sevilla-Callejo, M., Leunda, M., Santos, L., Franco-Múgica, F., Andrade, A., Carrión, J. S. and Valero-Garcés, B. L.: Strong continentality and effective moisture drove unforeseen vegetation dynamics since the last interglacial at inland Mediterranean areas: The Villarquemado sequence in NE Iberia, *Quat. Sci. Rev.*, 242, 106425, doi:10.1016/j.quascirev.2020.106425, 2020.

González, A. V. and Saa, M. P.: Pollen analyse of Holocene peat-bog in the Montes do Buio: Cuadramon (Galicia, N.W. of Spain, Quaternaire, 11(3–4), 257–267, doi:10.3406/quate.2000.1674, 2000.

Hannon, G. : Late Quaternary vegetation of Sanabria Marsh, North West Spain, Trinity College, Dublin, Ireland., 1985.

Hansen, M. and Song, X. P.: MEaSUREs Vegetation Continuous Fields (VCF) Yearly Global 0.05 Deg V001., NASA, L.

285 Process. Distrib. Act. Arch. Cent., doi:10.5067/MEaSUREs/VCF/VCF5KYR.001, 2018.

Janssen, C. R. and Woldringh, R. E.: A preliminary radiocarbon dated pollen sequence from the Serra da Estrela, Portugal., Finisterra, 16(32), 299–309, doi:10.18055/finis2176, 1981.

Jiménez-Moreno, G., García-Alix, A., Hernández-Corbán, M. D., Anderson, R. S. and Delgado-Huertas, A.: Vegetation, fire, climate and human disturbance history in the southwestern Mediterranean area during the late Holocene, Quat. Res., 290 79(2), 110–122, doi:10.1016/j.yqres.2012.11.008, 2013.

Julio Camarero, J., Sangüesa-Barreda, G., Pérez-Díaz, S., Montiel-Molina, C., Seijo, F. and López-Sáez, J. A.: Abrupt regime shifts in post-fire resilience of Mediterranean mountain pinewoods are fuelled by land use, Int. J. Wildl. Fire, 28(5), 329–341, doi:10.1071/WF18160, 2019.

295 Jung, M., Schwalm, C., Migliavacca, M., Walther, S., Camps-Valls, G., Koirala, S., Anthoni, P., Besnard, S., Bodesheim, P., Carvalhais, N., Chevallier, F., Gans, F., Goll, D. S., Haverd, V., Köhler, P., Ichii, K., Jain, A. K., Liu, J., Lombardozzi, D., Nabel, J. E. M. S., Nelson, J. A., O'sullivan, M., Pallandt, M., Papale, D., Peters, W., Pongratz, J., Rödenbeck, C., Sitch, S., Tramontana, G., Walker, A., Weber, U. and Reichstein, M.: Scaling carbon fluxes from eddy covariance sites to globe: synthesis and evaluation of the FLUXCOM approach, Biogeosciences, 17(5), 1343–1365, doi:10.5194/bg-17-1343-2020, 2020.

300 Kaal, J., Costa-Casais, M., Ferro-Vázquez, C., Pontevedra-Pombal, X. and Martínez-Cortizas, A.: Soil Formation of “Atlantic Rankers” from NW Spain—A High Resolution Aluminium and Iron Fractionation Study, Pedosphere, 18(4), 441–453, doi:10.1016/S1002-0160(08)60035-1, 2008.

305 Kaal, J., Carrión Marco, Y., Asouti, E., Martín Seijo, M., Martínez Cortizas, A., Costa-Casáis, M. and Criado-Boado, F.: Long-term deforestation in NW Spain: linking the Holocene fire history to vegetation change and human activities, Quat. Sci. Rev., 30, 161–175, doi:doi:10.1016/j.quascirev.2010.10.006, 2011.

Kaal, J., Criado-Boado, F., Costa-Casais, M., López-Sáez, J. A., López-Merino, L., Mighall, T., Carrión, Y., Silva Sánchez, N. and Martínez Cortizas, A.: Prehistoric land use at an archaeological hot-spot (the rock art park of Campo Lameiro, NW Spain) inferred from charcoal, synanthropic pollen and non-pollen palynomorph proxies, J. Archaeol. Sci., 40, 1518–1527, doi:doi:10.1016/j.jas.2012.09.024, 2013.

- 310 Klein Goldewijk, K., Beusen, A., Doelman, J. and Stehfest, E.: New anthropogenic land use estimates for the Holocene :  
HYDE 3.2, *Earth Syst. Sci. Data*, 9(2), 927–953, doi:<https://doi.org/10.5194/essd-2016-58>, 2017.
- van der Knaap, W. O. and van Leeuwen, J. F. N.: Holocene vegetation succession and degradation as responses to climatic change and human activity in the Serra de Estrela, Portugal, *Rev. Palaeobot. Palynol.*, 89(3–4), 153–211, doi:10.1016/0034-6667(95)00048-0, 1995.
- 315 van der Knaap, W. O. and van Leeuwen, J. F. N.: Late Glacial and early Holocene vegetation succession, altitudinal vegetation zonation, and climatic change in the Serra da Estrela, Portugal, *Rev. Palaeobot. Palynol.*, 97(3–4), 239–285, doi:10.1016/S0034-6667(97)00008-0, 1997.
- van der Knaap, W. O. and van Leeuwen, J.: Holocene vegetation, human impact, and climatic change in the Serra da Estrela, Portugal, *Diss. Bot.*, 234, 497–535, 1984.
- 320 Leunda, M., González-Sampériz, P., Gil-Romera, G., Aranbarri, J., Moreno, A., Oliva-Urcia, B., Sevilla-Callejo, M. and Valero-Garcés, B.: The Late-Glacial and Holocene Marboré Lake sequence (2612 m a.s.l., Central Pyrenees, Spain): Testing high altitude sites sensitivity to millennial scale vegetation and climate variability, *Glob. Planet. Change*, 157, 214–231, doi:10.1016/j.gloplacha.2017.08.008, 2017.
- Leunda, M., González-Sampériz, P., Gil-Romera, G., Bartolomé, M., Belmonte-Ribas, Á., Gómez-García, D., Kaltenrieder, P., Rubiales, J. M., Schwörer, C., Tinner, W., Morales-Molino, C. and Sancho, C.: Ice cave reveals environmental forcing of long-term Pyrenean tree line dynamics, *J. Ecol.*, 107(2), 814–828, doi:10.1111/1365-2745.13077, 2019.
- 325 Liu, M., Prentice, I. C., Ter Braak, C. J. F. and Harrison, S. P.: An improved statistical approach for reconstructing past climates from biotic assemblages: Improved palaeoclimate reconstruction, *Proc. R. Soc. A Math. Phys. Eng. Sci.*, 476(2243), doi:10.1098/rspa.2020.0346, 2020.
- 330 López-Merino, L., López-Sáez, J. A., Alba-Sánchez, F., Pérez-Díaz, S. and Carrión, J. S.: 2000 years of pastoralism and fire shaping high-altitude vegetation of Sierra de Gredos in central Spain, *Rev. Palaeobot. Palynol.*, 158(1–2), 42–51, doi:10.1016/j.revpalbo.2009.07.003, 2009.
- López-Merino, L., Cortizas, A. M. and López-Sáez, J. A.: Early agriculture and palaeoenvironmental history in the North of the Iberian Peninsula: a multi-proxy analysis of the Monte Areo mire (Asturias, Spain), *J. Archaeol. Sci.*, 37(8), 1978–1988,
- 335 doi:10.1016/j.jas.2010.03.003, 2010.
- López-Merino, L., Cortizas, A. M. and López-Sáez, J. A.: Human-induced changes on wetlands: A study case from NW Iberia, *Quat. Sci. Rev.*, 30(19–20), 2745–2754, doi:10.1016/j.quascirev.2011.06.004, 2011.
- López-Merino, L., Sánchez, N. S., Kaal, J., López-Sáez, J. A. and Cortizas, A. M.: Post-disturbance vegetation dynamics during the Late Pleistocene and the Holocene: An example from NW Iberia, *Glob. Planet. Change*, 92, 58–70, 2012.

- 340 López-Sáez, J. A., Sánchez, M. and López., P.: Evolución del Lanzahíta (Valle del Tiétar, vila) durante el Holoceno reciente: Una interpretación palinológica., Trasierra, 1999(4), 81–86, 1999.
- López-Sáez, J. A., López-García, P. and Cortés Sánchez, M.: Paleovegetación del Cuaternario reciente: Estudio arqueopalínológico, Cueva Bajondillo (Torremolinos). Secuencia cronocultural y paleoambiental del Cuaternario reciente en la Bahía Málaga, 139–156, 2007.
- 345 López-Sáez, J. A., López-Merino, L., Mateo, M. Á., Serrano, Ó., Pérez-Díaz, S. and Serrano, L.: Palaeoecological potential of the marine organic deposits of *Posidonia oceanica*: A case study in the NE Iberian Peninsula, *Palaeogeogr. Palaeoclimatol. Palaeoecol.*, 271(3–4), 215–224, doi:10.1016/j.palaeo.2008.10.020, 2009.
- López-Sáez, J. A., López-Merino, L., Alba-Sánchez, F., Pérez-Díaz, S., Abel-Schaad, D. and Carrión, J. S.: Late Holocene ecological history of *Pinus pinaster* forests in the Sierra de Gredos of central Spain, *Plant Ecol.*, 206(2), 195–209, 350 doi:10.1007/s11258-009-9634-z, 2010.
- López-Sáez, J. A., Abel-Schaad, D., Alba-Sánchez, F., González-Pellejero, R., Frochoso, M. and Allende, F.: 20. Culazón, Cantabrian Mountains (northern Spain), *Grana*, 52(4), 316–318, 2013.
- López-Sáez, J. A., Alba-Sánchez, F., Robles-López, S., Pérez-Díaz, S., Abel-Schaad, D., Sabariego-Ruiz, S. and Glais, A.: Exploring seven hundred years of transhumance, climate dynamic, fire and human activity through a historical mountain 355 pass in central Spain, *J. Mt. Sci.*, 13(7), 1139–1153, doi:10.1007/s11629-016-3885-7, 2016a.
- López-Sáez, J. A., Abel-Schaad, D., Robles-López, S., Pérez-Díaz, S., Alba-Sánchez, F. and Nieto-Lugilde, D.: Landscape dynamics and human impact on high-mountain woodlands in the western Spanish Central System during the last three millennia, *J. Archaeol. Sci. Reports*, 9, 203–218, doi:10.1016/j.jasrep.2016.07.027, 2016b.
- López-Sáez, J. A., Figueiral, I. and Cruz, D. J.: Palaeoenvironment and vegetation dynamics in Serra da Nave (Alto Paiva, 360 Beira Alta, Portugal) during the Late Pleistocene and the Holocene, in *Actas da Mesa-Redonda “A Pré-história e a Proto-história no Centro de Portugal: avaliação e perspectivas de futuro,”* edited by D. J. Cruz, Centro de Estudos Pré-históricos da Beira Alta, Viseu., 2017.
- López-Sáez, J. A., Pérez-Díaz, S., Rodríguez-Ramírez, A., Blanco-González, A., Villarías-Robles, J. J. R., Luelmo-Lautenschlaeger, R., Jiménez-Moreno, G., Celestino-Pérez, S., Cerrillo-Cuenca, E., Pérez-Asensio, J. N. and León, Á.: Mid-late Holocene environmental and cultural dynamics at the south-west tip of Europe (Doñana National Park, SW Iberia, 365 Spain), *J. Archaeol. Sci. Reports*, 22, 58–78, doi:10.1016/j.jasrep.2018.09.014, 2018a.
- López-Sáez, J. A., Vargas, G., Ruiz-Fernández, J., Blarquez, O., Alba-Sánchez, F., Oliva, M., Pérez-Díaz, S., Robles-López, S. and Abel-Schaad, D.: Paleofire dynamics in Central Spain during the Late Holocene: The role of climatic and anthropogenic forcing, *L. Degrad. Dev.*, 29(7), 2045–2059, doi:10.1002/ldr.2751, 2018b.

- 370 López-Sáez, J. A., Carrasco, R. M., Turu, V., Ruiz-Zapata, B., Gil-García, M. J., Luelmo-Lautenschlaeger, R., Pérez-Díaz, S., Alba-Sánchez, F., Abel-Schaad, D., Ros, X. and Pedraza, J.: Late Glacial-early holocene vegetation and environmental changes in the western Iberian Central System inferred from a key site: The Navamuño record, Béjar range (Spain), *Quat. Sci. Rev.*, 230, 106167, doi:10.1016/j.quascirev.2020.106167, 2020.
- 375 López Merino, L., López Sáez, J., Alba Sánchez, F., Pérez Díaz, S., Abel-Schaad, D. and Guerra Doce, E.: Estudio polínico de una laguna endorreica en Almenara de Adaja (Valladolid, Meseta Norte): cambios ambientales y actividad humana durante los últimos 2.800 años, *Rev. española Micropaleontol.*, 41(3), 333–347 [online] Available from: [https://digital.csic.es/bitstream/10261/93733/1/Estudio\\_polinico\\_laguna\\_endorreica.pdf](https://digital.csic.es/bitstream/10261/93733/1/Estudio_polinico_laguna_endorreica.pdf) (Accessed 22 March 2021), 2009.
- Luelmo-Lautenschlaeger, R., López-Sáez, J. A. and Pérez-Díaz, S.: 39. Las Lanchas, Toledo Mountains (central Spain), *Grana*, 57, 246–248, doi:10.1080/00173134.2017.1366547, 2018a.
- 380 Luelmo-Lautenschlaeger, R., López Sáez, J. A. and Pérez Díaz, S.: Contributions to the European Pollen Database. Botija, Toledo Mountains (central Spain), *Grana* 57 (4): 322- 324, 2018b.
- Luelmo-Lautenschlaeger, R., Pérez-Díaz, S., Alba-Sánchez, F., Abel-Schaad, D. and López-Sáez, J. A.: Vegetation history in the Toledo Mountains (central Iberia): human impact during the last 1300 years, *Sustainability*, 10(7), 2575, 2018c.
- 385 Luelmo-Lautenschlaeger, R., Blarquez, O., Pérez-Díaz, S., Morales-Molino, C. and López-Sáez, J. A.: The Iberian Peninsula’s Burning Heart—Long-Term Fire History in the Toledo Mountains (Central Spain), *Fire*, 2(4), 54, 2019a.
- Luelmo-Lautenschlaeger, R., Pérez-Díaz, S., Blarquez, O., Morales-Molino, C. and López-Sáez, J. A.: The Toledo Mountains: A Resilient landscape and a landscape for resilience? Hazards and strategies in a mid-elevation mountain region in Central Spain, *Quaternary*, 2(4), 35, 2019b.
- 390 Manzano, S., Carrión, J. S., López-Merino, L., Jiménez-Moreno, G., Toney, J. L., Armstrong, H., Anderson, R. S., García-Alix, A., Pérez, J. L. G. and Sánchez-Mata, D.: A palaeoecological approach to understanding the past and present of Sierra Nevada, a Southwestern European biodiversity hotspot, *Glob. Planet. Change*, 175, 238–250, doi:10.1016/j.gloplacha.2019.02.006, 2019.
- Mariscal Alvarez, B.: Estudio polínico de la turbera del Cueto de la Avellanosa, Polaciones (Cantabria). VI Reunion do grupo español de trabalho de Quaternario, *Cuad. do Lab. xeoloxico laxe*, 5, 205–226, 1983.
- 395 Mariscal Alvarez, B.: Análisis polínico de la turbera del Pico del Sertal, de la Sierra de Paña Sagra. Reconstrucción de la paleoflora y de la paleoclimatología durante el Holoceno en la zona central de la Cordillera Cantábrica, *Quat. Clim. West. Mediterr.* Madrid Univ. Autónoma, 1986.
- Mariscal, B.: Comparacion palinologica entre una turbera de la cordillera central y unas turberas de la cordillera cantabrica, in II. European Paleobot, p. 28, Universidad Complutense Madrid., 1989.

- 400 Mariscal, B.: Variación de la vegetación holocena (4300-280 B.P.) de Cantabria a traves del análisis polínico de la turbera del Alsa, *Estud. geológicos*, 49(1), 63–69, doi:10.3989/egeol.93491-2338, 1993.
- Martín-Puertas, C., Valero-Garcés, B. L., Pilar Mata, M., González-Sampériz, P., Bao, R., Moreno, A. and Stefanova, V.: Arid and humid phases in southern Spain during the last 4000 years: the Zoñar Lake record, *Córdoba, The Holocene*, 18(6), 907–921, doi:10.1177/0959683608093533, 2008.
- 405 Martínez Cortizas, A., García-Rodeja, E., Pontevedra Pombal, X., Nóvoa Muñoz, J. C., Weiss, D. and Cheburkin, A.: Atmospheric Pb deposition in Spain during the last 4600 years recorded by two ombrotrophic peat bogs and implications for the use of peat as archive, *Sci. Total Environ.*, 292(1–2), 33–44, doi:10.1016/S0048-9697(02)00031-1, 2002.
- McKeever, M.: Comparative palynological studies of two lake sites in western Ireland and northwestern Spain., *Trinity College, Dublin, Ireland.*, 1984.
- 410 Mighall, T. M., Martínez Cortizas, A., Biester, H. and Turner, S. E.: Proxy climate and vegetation changes during the last five millennia in NW Iberia: Pollen and non-pollen palynomorph data from two ombrotrophic peat bogs in the North Western Iberian Peninsula, *Rev. Palaeobot. Palynol.*, 141(1–2), 203–223, doi:10.1016/j.revpalbo.2006.03.013, 2006.
- Miras, Y., Ejarque, A., Riera, S., Palet, J. M., Orengo, H. and Euba, I.: Dynamique holocène de la végétation et occupation des Pyrénées andorraines depuis le Néolithique ancien, d’après l’analyse pollinique de la tourbière de Bosc dels Estanyons  
415 (2180 m, Vall del Madriu, Andorre), *Comptes Rendus Palevol*, 6(4), 291–300, 2007.
- Miras, Y., Ejarque, A., Orengo, H., Mora, S. R., Palet, J. M. and Poiraud, A.: Prehistoric impact on landscape and vegetation at high altitudes: An integrated palaeoecological and archaeological approach in the eastern Pyrenees (Perafita valley, Andorra), *Plant Biosyst.*, 144(4), 924–939, doi:10.1080/11263504.2010.491980, 2010.
- Miras, Y., Ejarque, A., Riera Mora, S., Orengo, H. A. and Palet Martinez, J. M.: 28. Andorran high Pyrenees (Perafita Valley, Andorra): SerraMijtana fen, *Grana*, 54(4), 313–316, doi:10.1080/00173134.2015.1087590, 2015.
- 420 Moe, D. and Van Der Knaap, W. O.: Transhumance in mountain areas : Additional interpretation of three pollen diagrams from Norway, Portugal and Switzerland, *Pact*, (31), 91–103, 1990.
- Morales-Molino, C. and García-Antón, M.: Vegetation and fire history since the last glacial maximum in an inland area of the western Mediterranean Basin (Northern Iberian Plateau, NW Spain), *Quat. Res.*, 81(1), 63–77,  
425 doi:10.1016/j.yqres.2013.10.010, 2014.
- Morales-Molino, C., García Antón, M. and Morla, C.: Late Holocene vegetation dynamics on an Atlantic-Mediterranean mountain in NW Iberia, *Palaeogeogr. Palaeoclimatol. Palaeoecol.*, 302(3–4), 323–337, doi:10.1016/j.palaeo.2011.01.020, 2011.

Morales-Molino, C., García-Antón, M., Postigo-Mijarra, J. M. and Morla, C.: Holocene vegetation, fire and climate

430 interactions on the westernmost fringe of the Mediterranean Basin, *Quat. Sci. Rev.*, 59, 5–17,  
doi:10.1016/j.quascirev.2012.10.027, 2013.

Morales-Molino, C., Colombaroli, D., Valbuena-Carabaña, M., Tinner, W., Salomón, R. L., Carrión, J. S. and Gil, L.: Land-use history as a major driver for long-term forest dynamics in the Sierra de Guadarrama National Park (central Spain) during the last millennia: implications for forest conservation and management, *Glob. Planet. Change*, 152, 64–75,

435 doi:10.1016/j.gloplacha.2017.02.012, 2017a.

Morales-Molino, C., Tinner, W., García-Antón, M. and Colombaroli, D.: The historical demise of *Pinus nigra* forests in the Northern Iberian Plateau (south-western Europe), edited by M. McGlone, *J. Ecol.*, 105(3), 634–646, doi:10.1111/1365-2745.12702, 2017b.

Morales-Molino, C., Colombaroli, D., Tinner, W., Perea, R., Valbuena-Carabaña, M., Carrión, J. S. and Gil, L.: Vegetation  
440 and fire dynamics during the last 4000 years in the Cabañeros National Park (central Spain), *Rev. Palaeobot. Palynol.*, 253,  
110–122, doi:10.1016/j.revpalbo.2018.04.001, 2018.

Morales-Molino, C., Tinner, W., Perea, R., Carrión, J. S., Colombaroli, D., Valbuena-Carabaña, M., Zafra, E. and Gil, L.: Unprecedented herbivory threatens rear-edge populations of *Betula* in southwestern Eurasia, *Ecology*, 100(11),  
doi:10.1002/ecy.2833, 2019.

445 Morellón, M., Valero-Garcés, B., González-Sampériz, P., Vegas-Vilarrúbia, T., Rubio, E., Rieradevall, M., Delgado-Huertas, A., Mata, P., Romero, Ó., Engstrom, D. R., López-Vicente, M., Navas, A. and Soto, J.: Climate changes and human activities recorded in the sediments of Lake Estanya (NE Spain) during the Medieval Warm Period and Little Ice Age, *J. Paleolimnol.*, 46(3), 423–452, doi:10.1007/s10933-009-9346-3, 2011.

Moreno, A., López-Merino, L., Leira, M., Marco-Barba, J., Penélope González-Sampériz, •, Blas, •, Valero-Garcés, L.,  
450 Antonio López-Sáez, J., Santos, L., Mata, P., Ito, E., López-Sáez, J. A., Leira, M., Santos, Á. L., Santos, L., Marco-Barba, J., Mata, P., Moreno, A., Ito, E., González-Sampériz, Á. P., Valero-Garcés, B. L., González-Sampériz, P. and López-Merino, L.: Revealing the last 13,500 years of environmental history from the multiproxy record of a mountain lake (Lago Enol, northern Iberian Peninsula), *J Paleolimnol.*, 46, 327–349, doi:10.1007/s10933-009-9387-7, 2011.

Múgica, F. F., Antón, M. G., Ruiz, J. M., Juaristi, C. M. and Ollerol, H. S.: The Holocene history of *Pinus* forests in the  
455 Spanish Northern Meseta, *The Holocene*, 11(3), 343–358, doi:10.1191/095968301669474913, 2001.

Obiol, R. i and Roure, J.: Análisis polínico de una secuencia holocénica en Roquetas de Mar (Almería), in *Trabajos de Palinología básica y aplicada: X Simposio de Palinología*, (APLE, Valencia, septiembre 1994), pp. 189–198, Universitat de València. [online] Available from: <https://dialnet.unirioja.es/servlet/articulo?codigo=1387752> (Accessed 23 March 2021), 1994.

- 460 Pantaléon-Cano, J., Yll, E.-I., Pérez-Obiol, R. and Roure, J. M.: Palynological evidence for vegetational history in semi-arid areas of the western Mediterranean (Almería, Spain), *The Holocene*, 13(1), 109–119, doi:10.1191/0959683603hl598rp, 2003.
- Penalba, M. C.: The history of the Holocene vegetation in Northern Spain from pollen analysis, *J. Ecol.*, 82(4), 815, doi:10.2307/2261446, 1994.
- 465 Penalba, M. C. and Garmendia, M. P.: Dynamique de végétation tardiglaciaire et holocène du Centre-Nord de l’Espagne d’après l’analyse pollinique, Aix-Marseille 3, January. [online] Available from: <https://www.theses.fr/1989AIX30033> (Accessed 22 March 2021), 1989.
- Pérez-Díaz, S. and López-Sáez, J. A.: 33. Verdeospesoa mire (Basque Country, Northern Iberian Peninsula, Spain), *Grana*, 56(4), 315–317, doi:10.1080/00173134.2016.1271824, 2017.
- 470 Pérez-Díaz, S. and López-Sáez, J. A.: The Western Pyrenean (Northern Iberian Peninsula) during the Upper Paleolithic: A Palaeoenvironmental Approach, in *Human Adaptations to the Last Glacial Maximum: The Solutrean and its Neighbors*, edited by J. Schmidt, I., Cascalheira and G.-C. Bicho, N., Weniger., 2019.
- Pérez-Díaz, S., López-Sáez, J. A., Núñez de la Fuente, S. and Ruiz-Alonso, M.: Early farmers, megalithic builders and the shaping of the cultural landscapes during the Holocene in Northern Iberian mountains. A palaeoenvironmental perspective, *J. Archaeol. Sci. Reports*, 18, 463–474, doi:10.1016/j.jasrep.2018.01.043, 2018.
- 475 Pérez-Obiol, R., Bal, M. C., Pèlachs, A., Cunill, R. and Soriano, J. M.: Vegetation dynamics and anthropogenically forced changes in the Estanilles peat bog (southern Pyrenees) during the last seven millennia, *Veg. Hist. Archaeobot.*, 21(4–5), 385–396, doi:10.1007/s00334-012-0351-5, 2012.
- Pérez-Obiol, R. and Julià, R.: Climatic change on the iberian peninsula recorded in a 30,000-yr pollen record from lake Banyoles, *Quat. Res.*, 41(1), 91–98, doi:10.1006/qres.1994.1010, 1994.
- 480 Pérez-Sanz, A., González-Sampériz, P., Moreno, A., Valero-Garcés, B., Gil-Romera, G., Rieradevall, M., Tarrats, P., Lasheras-Álvarez, L., Morellón, M. and Belmonte, A.: Holocene climate variability, vegetation dynamics and fire regime in the central Pyrenees: the Basa de la Mora sequence (NE Spain), *Quat. Sci. Rev.*, 73, 149–169, 2013.
- Ramos-Román, M. J., Jiménez-Moreno, G., Anderson, R. S., García-Alix, A., Toney, J. L., Jiménez-Espejo, F. J. and Carrión, J. S.: Centennial-scale vegetation and North Atlantic Oscillation changes during the Late Holocene in the southern Iberia, *Quat. Sci. Rev.*, 143, 84–95, doi:10.1016/j.quascirev.2016.05.007, 2016.
- 485 Revelles, J., Cho, S., Iriarte, E., Burjachs, F., van Geel, B., Palomo, A., Piqué, R., Peña-Chocarro, L. and Terradas, X.: Mid-Holocene vegetation history and Neolithic land-use in the Lake Banyoles area (Girona, Spain), *Palaeogeogr. Palaeoclimatol. Palaeoecol.*, 435, 70–85, doi:10.1016/j.palaeo.2015.06.002, 2015.

- 490 Revelles, J., Burjachs, F., Palomo, A., Piqué, R., Iriarte, E., Pérez-Obiol, R. and Terradas, X.: Human-environment interaction during the Mesolithic- Neolithic transition in the NE Iberian Peninsula. Vegetation history, climate change and human impact during the Early-Middle Holocene in the Eastern Pre-Pyrenees, *Quat. Sci. Rev.*, 184, 183–200, doi:10.1016/j.quascirev.2017.08.025, 2018.
- 495 Riera-Mora, S. and Esteban-Amat, A.: Vegetation history and human activity during the last 6000 years on the central Catalan coast (northeastern Iberian Peninsula), *Veg. Hist. Archaeobot.*, 3(1), doi:10.1007/BF00208885, 1994.
- Robles-López, S., Luelmo-Lautenschlaeger, R., Pérez-Díaz, S., Abel-Schaad, D., Alba-Sánchez, F., Ruiz-Alonso, M. and López-Sáez, J. A.: Vulnerabilidad y resiliencia de los pinares de alta montaña de la Sierra de Gredos (Ávila, Sistema Central): dos mil años de dinámica socioecológica, *Cuaternario y Geomorfol.*, 31(3–4), 51, doi:10.17735/cyg.v31i3-4.55594, 2017.
- 500 Robles-López, S., Fernández Martín-Consuegra, A., Pérez-Díaz, S., Alba-Sánchez, F., Broothaerts, N., Abel-Schaad, D. and López-Sáez, J. A.: The dialectic between deciduous and coniferous forests in central Iberia: A palaeoenvironmental perspective during the late Holocene in the Gredos range, *Quat. Int.*, 470, 148–165, doi:10.1016/j.quaint.2017.05.012, 2018.
- Robles-López, S., Manzano-Rodríguez, S., Pérez-Díaz, S. and López-Sáez, J. A.: 35. Labradillos mire, Gregos Range (central Spain), *Grana*, 56(5), 398–400, doi:10.1080/00173134.2017.1282976, 2017.
- 505 Robles-López, S., Pérez-Díaz, S., Ruiz-Alonso, M., Blarquez, O., Luelmo-Lautenschlaeger, R. and López-Sáez, J. A.: Holocene vegetation and fire dynamics in the supra-Mediterranean belt of the Gredos Range (central Iberian Peninsula), *Plant Biosyst. - An Int. J. Deal. with all Asp. Plant Biol.*, 154(1), 74–86, doi:10.1080/11263504.2019.1578281, 2020.
- Salonen, J. S., Ilvonen, L., Seppä, H., Holmström, L., Telford, R. J., Gaidamavičius, A., Stančikaitė, M. and Subetto, D.: Comparing different calibration methods (WA/WA-PLS regression and Bayesian modelling) and different-sized calibration sets in pollen-based quantitative climate reconstruction, *Holocene*, 22(4), 413–424, doi:10.1177/0959683611425548, 2012.
- 510 Sanchez Goñi, M. F. S. and Hannon, G. E.: High-altitude vegetational pattern on the Iberian Mountain Chain (north-central Spain) during the Holocene, *The Holocene*, 9(1), 39–57, doi:10.1191/095968399671230625, 1999.
- Schneider, H., Höfer, D., Trog, C., Busch, S., Schneider, M., Baade, J., Daut, G. and Mäusbacher, R.: Holocene estuary development in the Algarve Region (Southern Portugal) – A reconstruction of sedimentological and ecological evolution, *Quat. Int.*, 221(1–2), 141–158, doi:10.1016/j.quaint.2009.10.004, 2010.
- Schneider, H., Höfer, D., Trog, C. and Mäusbacher, R.: Holocene landscape development along the Portuguese Algarve coast - A high resolution palynological approach, *Quat. Int.*, 407, 47–63, doi:10.1016/j.quaint.2016.02.039, 2016.

Silva-Sánchez, N., Martínez Cortizas, A., Abel-Schaad, D., López-Sáez, J. A. and Mighall, T. M.: Influence of climate change and human activities on the organic and inorganic composition of peat during the ‘Little Ice Age’(El Payo mire, W Spain), *The Holocene*, 26(8), 1290–1303, 2016.

Stefanini, B. : A comparison of climate and vegetation dynamics in central Ireland and NW Spain since the mid-Holocene, University of Dublin, Trinity College, Dublin, Leinster, Ireland., 2008.

Stevenson, A. C.: The Holocene forest history of the Montes Universales, Teruel, Spain, *The Holocene*, 10(5), 603–610, doi:10.1191/095968300670543500, 2000.

Turner, C. and Hannon, G. E.: Vegetational evidence for late Quaternary climatic changes in southwest Europe in relation to the influence of the North Atlantic Ocean, *Philos. Trans. R. Soc. London. B, Biol. Sci.*, 318(1191), 451–485, 1988.

Turu, V., Carrasco, R. M., Pedraza, J., Ros, X., Ruiz-Zapata, B., Soriano-López, J. M., Mur-Cacuho, E., Pélachs-Mañosa, A., Muñoz-Martín, A., Sánchez, J. and Echeverría-Moreno, A.: Late glacial and post-glacial deposits of the Navamuño peatbog (Iberian Central System): Chronology and paleoenvironmental implications, *Quat. Int.*, 470, 82–95,

doi:doi:10.1016/j.quaint.2017.08.018, 2018.

Valero-Garcés, B. L., González-Sampériz, P., Gil-Romera, G., Benito, B. M., Moreno, A., Oliva-Urcia, B., Aranbarri, J., García-Prieto, E., Frugone, M., Morellón, M., Arnold, L. J., Demuro, M., Hardiman, M., Blockley, S. P. E. and Lane, C. S.: A multi-dating approach to age-modelling long continental records: The 135 ka El Cañizar de Villarquemado sequence (NE Spain), *Quat. Geochronol.*, 54, 101006, doi:10.1016/j.quageo.2019.101006, 2019.

Valero-Garcés, B. L., Navas, A., Machin, J., Stevenson, T. and Davis, B.: Responses of a saline lake ecosystem in a semiarid region to irrigation and climate variability: The history of Salada Chiprana, central Ebro basin, Spain., 2000.

Viovy, N.: CRUNCEP Version 7 - Atmospheric Forcing Data for the Community Land Model, Res. Data Arch. Natl. Cent. Atmos. Res. Comput. Inf. Syst. Lab., doi:10.5065/PZ8F-F017, 2018.

Yll, E. I., Pérez-Obiol, R., Pantaleón-Cano, J. and Roure, J. M.: Dinámica del paisaje vegetal en la vertiente mediterránea de la Península Ibérica e Islas Baleares desde el Tardiglaciado hasta el presente, Reconstrucción Paleoambientes y cambios climáticos durante el Cuaternario, 3, 319–328, 1995.